CLARKSON UNIVERSITY

Nonequilibrium Models for Multiphase Separation Processes

A Dissertation
by
Miaozhen Lao

Department of Chemical Engineering

Submitted in partial fulfillment of the requirements

for the degree of

Doctor of Philosophy

(Chemical Engineering)

September, 1989

Accepted by the Graduate School

Date Dean

Contents

Chapter 3

A Nonequilibrium Model for Liquid-Liquid Extraction

3.1 Introduction

Liquid-liquid extraction belongs to the class of diffusional separation processes and one that is gaining in importance. Models of the liquid-liquid extraction process are many and varied, ranging from simple (or not so simple) equilibrium stage models described in Chapter 1 to complicated kinetic models based on models of the flow and mass transfer characteristics of liquid liquid dispersions (see, for example, Treybal (1963), Skelland (1974), and Pratt (1983) for reviews).

The equilibrium stage model of extraction suffers from the same shortcomings that the equilibrium stage model of distillation and absorption processes possesses because the process rarely operates at equilibrium. One way of dealing with situations like this is through the use of stage or overall efficiencies. There are many papers that deal with the efficiency problem (see Lo, Baird and Hanson (1983) for a summary). Methods of choosing the efficiency to use in liquid-liquid extraction cover the entire spectrum from simply picking a number to sophisticated methods such as that of Rocha et al. (1986).

This chapter describes a nonequilibrium model of liquid-liquid extraction and presents results of simulations of four extraction operations in sieve tray columns for which experimental data is available. The model described in this chapter is, perhaps, closest in spirit to that of Skelland and Conger (1973) and Skelland (1974), but the mass transfer models that we have used and the methods of solving the model equations are, however, quite different.

3.2 Theoretical Model for Liquid-Liquid Extraction

The sieve tray column is one of the most common type of extractors used in liquid-liquid extraction. A schematic diagram of a sieve stage in a liquid-liquid extraction column is shown in Figure 3.1. Liquid from the stage below is brought into

contact with liquid from the stage above and allowed to exchange mass across their common interface represented in the Figure 3.2 by the wavy line. Provision may also be made for feed and/or withdrawal of either phase. A complete extraction column is taken to consist of a sequence of stages. The equations used to model the behavior of this stage/section of a column include the mass balances for each phase, equations that model the rate at which mass is transferred from one phase to another and equations that express the assumption that equilibrium between the two phases exists at (and *only* at) the interface. The energy balance and energy transfer rate equations can be *ignored* in the simulation of liquid-liquid extraction process, because the temperature change in this process is *negligible*. The model equations are presented below.

3.2.1 The Conservation Equations

There are c component material balances for each phase

$$\begin{aligned} \mathtt{M}'_{ij} \equiv\ & (1 + s'_j - B'_j)L'_j x'_{ij} - (1 - B'_{j+1})L'_{j+1} x'_{i,j+1} \\ & -F'_j z'_{ij} + N'_{ij} a_j = 0 \end{aligned} \tag{3.1}$$

$$\begin{aligned} \mathtt{M}''_{ij} \equiv\ & (1 + s''_j - B''_j)L''_j x''_{ij} - (1 - B''_{j-1})L''_{j-1} x''_{i,j-1} \\ & -F''_j z''_{ij} - N''_{ij} a_j = 0 \end{aligned} \tag{3.2}$$

The s_j are the ratios of sidestream to interstage flow rates and B_j are the backmixing flow ratios (the terms expressing backflow of the two phases are not part of the nonequilibrium model for distillation and absorption in Chapter 2).

The last term in Equations (3.1-3.2) expresses the rate of mass transfer from one phase to the other: a_j is the interfacial area per stage, N'_{ij} and N''_{ij} represent the

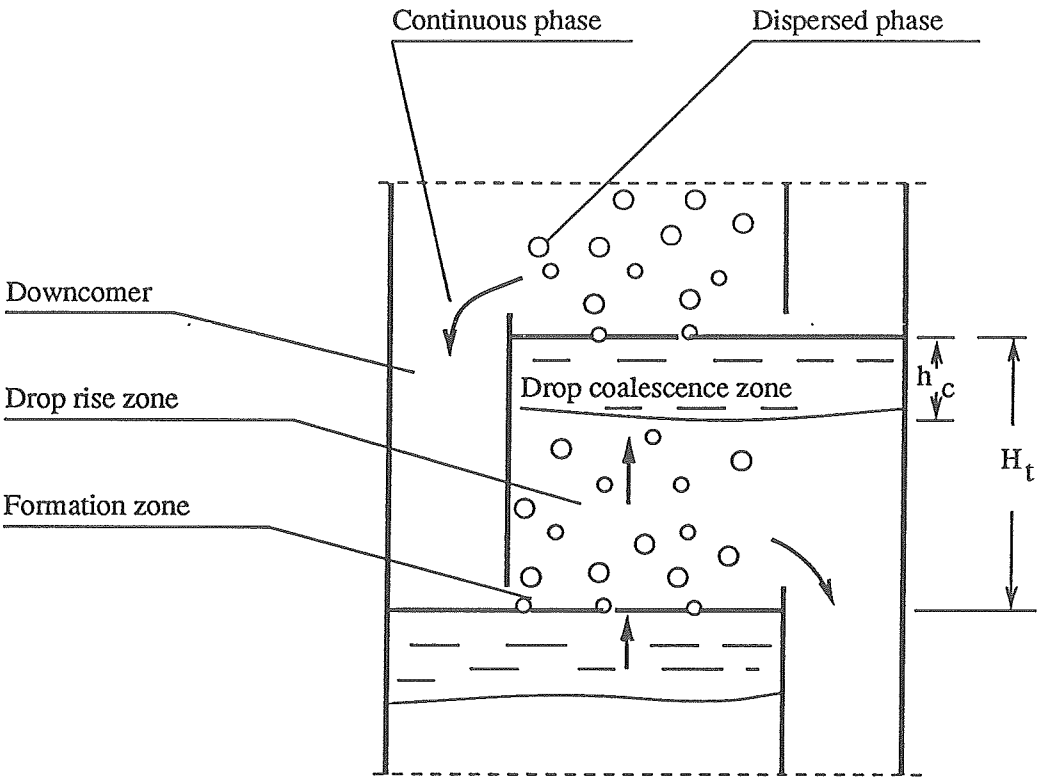

Figure 3.1: Liquid-liquid extraction in a sieve tray column.

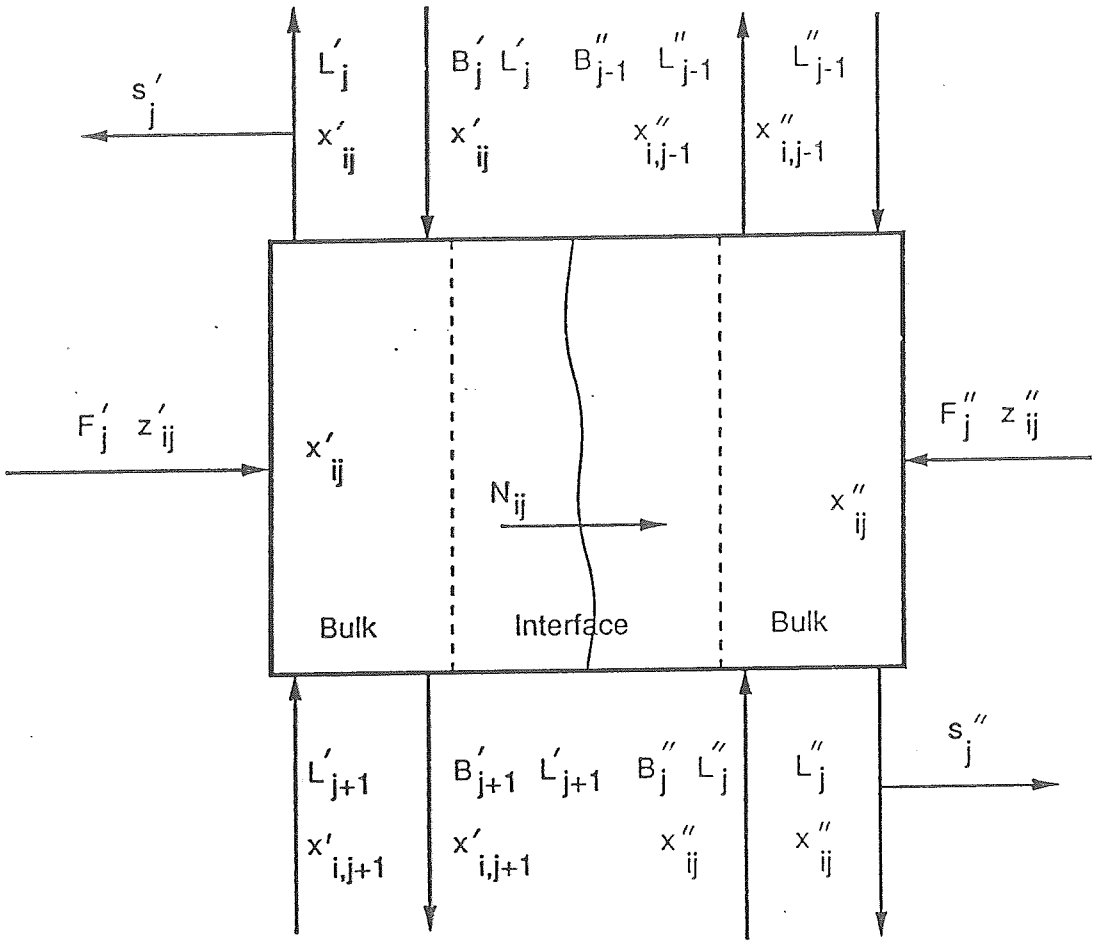

Figure 3.2: Schematic diagram of a nonequilibrium stage for liquid-liquid extraction.

interphase molar fluxes of species i from the $'$ and to the $''$ phase, respectively, in the stage j. We have used a single term to represent what in an actual simulation may be the sum of several contributions to the overall mass transfer rate. More on this topic below.

The total material balances for the two phases are obtained by summing up the component balances

$$\mathtt{M}'_{tj} \equiv (1 + s'_j - B'_j)L'_j - (1 - B'_{j+1})L'_{j+1} - F'_j + N'_{tj}a_j = 0 \tag{3.3}$$

$$\mathtt{M}''_{tj} \equiv (1 + s''_j - B''_j)L''_j - (1 - B''_{j-1})L''_{j-1} - F''_j - N''_{tj}a_j = 0 \tag{3.4}$$

where N_t is the total molar flux.

The conservation equations for each phase are linked by material balances around the interface:

$$\mathtt{M}^I_{ij} \equiv N'_{ij} - N''_{ij} = 0 \qquad \mathtt{M}^I_{tj} \equiv N'_{tj} - N''_{tj} = 0 \tag{3.5}$$

Equations (3.1-3.5) may be combined to give the conservation equations for the stage as a whole, the equations that are used in equilibrium stage simulation.

3.2.2 Mass Transfer Rate Equations

The molar fluxes are made up of a diffusive contribution and a convective term

$$N'_i = J'_i + x'_i N'_t = N_i = J''_i + x''_i N''_t = N''_i \tag{3.6}$$

The diffusion fluxes in either phase are given by a relation of the form

$$(J) = c_t[k^\circ](\Delta x) \tag{3.7}$$

where $[k^{\circ}]$ is a matrix (order $c-1$) of multicomponent mass transfer coefficients. (Δx) is a column matrix of driving forces. If we adopt the convention that transfers from the $'$ phase to the $''$ phase are positive then $(\Delta x') = (\bar{x}' - x'^{I})$ and $(\Delta x'') = (x''^{I} - \bar{x}'')$, where $\bar{x}$ is the average bulk composition and x^{I} is the interface composition.

To calculate the matrices of multicomponent mass transfer coefficients we have used the method of Krishna (1977) in which $[k^{\circ}]$ is related to *binary pair* mass transfer coefficients through a solution of the Generalized Maxwell-Stefan equations for a film model of mass transfer. In this method the matrix $[k^{\circ}]$ is calculated from

$$[k^{\circ}] = [R]^{-1}[\Gamma][\Theta] \tag{3.8}$$

The matrix $[R]$ can be calculated from Equation (2.14). $[\Gamma]$ is a matrix of thermodynamic factors as defined as Equation (2.15). $[\Theta]$ is a matrix of correction factors that accounts for the influence of the mass transfer rates on the mass transfer coefficients

$$[\Theta'] = [\theta'][exp[\theta'] - [I]]^{-1} \tag{3.9}$$

$$[\Theta''] = [\theta'']exp[\theta''][exp[\theta''] - [I]]^{-1} \tag{3.10}$$

where $[\theta]$ is defined by

$$[\theta] = [\Gamma]^{-1}[\Phi] \tag{3.11}$$

The matrix $[\Phi]$ has elements

$$\Phi_{ii} = \frac{N_i}{c_t k_{ic}} + \sum_{\substack{l=1 \\ l \neq i}}^{c} \frac{N_l}{c_t k_{il}}$$

$$\Phi_{ij} = -\frac{N_i}{c_t}\left(\frac{1}{k_{ij}} - \frac{1}{k_{ic}}\right) \tag{3.12}$$

There have not been many previous attempts to use a matrix formulation of mass transfer in multicomponent systems to simulate entire extraction columns. To the best of our knowledge, the only other paper to attempt this (although in quite a different way) is by Negri and Korchinsky (1986). Krishna et al. (1985) have used a matrix model of mass transfer to interpret experimental data in a batch (Lewis) extraction cell.

3.2.3 Interface Model

The familiar equations of liquid-liquid equilibrium are used to relate the compositions *at the interface*

$$\mathbb{Q}_{ij}^{I} \equiv K_{ij} x_{ij}^{\prime\prime I} - x_{ij}^{\prime I} = 0 \tag{3.13}$$

where $K_{ij} = K_{ij}(x_{ij}^{\prime I}, x_{ij}^{\prime\prime I})$ are the equilibrium ratios calculated as the ratio of activity coefficients (Henley and Seader, 1981)

$$K_i = \gamma_i^{\prime\prime} / \gamma_i^{\prime} \tag{3.14}$$

3.3 Solving the Model Equations

There is a total of $5c$ independent variables and $5c$ equations per stage. As in our previous work with nonequilibrium models we use Newton's method. Newton's method has been used to solve equilibrium stage models of extraction by, for example, Roche (1971) and Warner and Harris (1987).

In this application of Newton's method (see Equation 2.25) (F) is defined as

$$(F)^T \equiv \left((F_1)^T, (F_2)^T \cdots, (F_s)^T\right)$$

where the vector of functions for the j-th stage (F_j) is

$$\begin{aligned}(F_j)^T \equiv\ & (\mathtt{M}'_{tj}, \mathtt{M}'_{1j}, \mathtt{M}'_{2j} \cdots, \mathtt{M}'_{cj}, \mathtt{M}''_{tj}, \mathtt{M}''_{1j}, \mathtt{M}''_{2j} \cdots, \mathtt{M}''_{cj}, \\ & \mathtt{R}'_{1j}, \mathtt{R}'_{2j} \cdots, \mathtt{R}'_{c-1,j}, \mathtt{Q}^I_{1j}, \mathtt{Q}^I_{2j} \cdots, \mathtt{Q}^I_{cj}, \mathtt{R}''_{1j}, \mathtt{R}''_{2j} \cdots, \mathtt{R}''_{c-1,j})\end{aligned}$$

and (X) is defined by

$$(X)^T \equiv \left((X_1)^T, (X_2)^T \cdots, (X_s)^T\right)$$

with (X_j), the vector of variables for the j-th stage, defined as

$$\begin{aligned}(X_j)^T \equiv\ & (L'_j, x'_{1j}, x'_{2j} \cdots, x'_{cj}, L''_j, x''_{1j}, x''_{2j} \cdots, x''_{cj}, N_{1j}, N_{2j} \cdots, N_{cj}, \\ & x'^I_{1j}, x'^I_{2j} \cdots, x'^I_{c-1,j} x''^I_{1j}, x''^I_{2j} \cdots, x''^I_{c-1,j})\end{aligned}$$

The R-equations are Equations (3.6 and 3.7) written in the form

$$(\mathtt{R}'_j) \equiv (N_j) - N_{tj}(\bar{x}'_j) - c'_{tj}[k^{*\prime}_j](\bar{x}'_j - x'^I_j) = (0) \tag{3.15}$$

$$(\mathtt{R}''_j) \equiv (N_j) - N_{tj}(\bar{x}''_j) - c''_{tj}[k^{*\prime\prime}_j](x''^I_j - \bar{x}''_j) = (0) \tag{3.16}$$

For simplicity only one term is included in equations (3.15 and 3.16) when in practice there may be two or three independent contributions to the total mass transfer rate.

3.4 Application to Sieve Tray Columns

In a sieve tray extraction column, one liquid phase becomes dispersed in the continuous liquid phase as it passes through the perforations of the tray. The continuous liquid phase moves across the tray. Three regions for mass transfer have been

identified: the drop formation zone, the drop rise or fall zone, and the drop coalescence zone (see, for example, Rocha, 1984). An illustration of these three zones is provided in Figure 3.1. Axial mixing in sieve tray columns is not significant (Treybal, 1963; Eldridge et al., 1986). The backmixing terms were, therefore, set to zero for our simulations.

3.5 Flow Regimes

In a sieve tray extractor, mass transfer occurs in the three regions described as follow:

1. The drop formation zone

   The drops form when the dispersed liquid phase passes through perforations on the tray.

2. The drop rise/fall zone

   Above the drop formation region, liquid drops of all shapes and sizes rise or fall through the cross-flowing continuous liquid phase.

3. The drop coalescence zone

   Coalescence of drops under the tray above the light phase dispersed (or on the top of the tray below the heavy phase dispersed) occurs in this region, two liquid phases, consequently, separate and then go to the upper (or lower) stage. The contribution of this mechanism to the total mass transfer process appears to be quite small, sometimes the value taken as an average approximated as 10% of the drop formation, and is very often neglected.

3.6 Mass Transfer Coefficients

Correlations of mass transfer coefficients for sieve tray extractors have been reviewed by Skelland (1974, 1979) and Treybal (1980). More recently, Rocha et al. (1984 and 1986) have presented a model for the mass transfer efficiency of sieve tray extractors. The generalized model for calculating mass transfer coefficients presented in their paper is summarized below.

(1) For drop formation region

$$k_f^D = (-6.0 + 0.07We + 6.5\frac{\sigma_{ref}}{\sigma_{syst}})\frac{\rho^D}{c_t^D M^D}\sqrt{\frac{D^D U_0}{d_p}} \tag{3.17}$$

$$k_f^C = (-6.0 + 0.07We + 6.5\frac{\sigma_{ref}}{\sigma_{syst}})\frac{\rho^C}{c_t^C M^C}\sqrt{\frac{D^C U_0}{d_p}} \tag{3.18}$$

where U_0 is the velocity through orifice, i.e. hole velocity. The superscripts D and C represent the dispersed and continuous phases respectively. We is the Weber number defined as

$$We = \frac{d_h U_0^2 \rho^D}{\sigma g_c} \tag{3.19}$$

where

$$\sigma_{ref} = 35 \qquad dynes/cm$$

(2) Drop rise/fall region

$$k_r^D = (0.70 + 0.02We)\frac{\rho^D}{c_t^D M^D}(\frac{0.00375U_s}{1 + \frac{\mu^D}{\mu^C}}) \tag{3.20}$$

$$k_r^C = 0.725(0.70 + 0.02We)\frac{\rho^C}{c_t^C M^C}\left(\frac{d_p U_s \rho^C}{\mu^C}\right)^{-0.43}\left(\frac{\mu^C}{\rho^C D^C}\right)^{-0.58}(1-\phi)U_s \qquad (3.21)$$

where the slip velocity (relative velocity), U_s, is given by

$$U_s = \frac{U^D}{\phi} + \frac{U^C}{1-\phi} \qquad (3.22)$$

$$\phi = \frac{volume\ of\ dispersed\ phase\ drops}{volume\ of\ both\ phases} \qquad (3.23)$$

(3) Interfacial area

The total interfacial area for drop formation zone is

$$A_f = N_p \pi d_p^2 \qquad (3.24)$$

The total interfacial area for drop rise zone is

$$A_r = \frac{6\phi}{d_p}(A_{col} - A_{dow})(H_t - h_c) \qquad (3.25)$$

where $H_t - h_c$ is liquid holdup on the tray. H_t is the tray spacing and h_c is the height of the coalesced layer determined by Major and Hertog, (1955).

$$h_c = \frac{\rho^D U_0^2}{2\Delta\rho g}\left(1 - \frac{0.71}{\ln Re}\right)^{-2} + \frac{2.47\rho^C U_{dow}^2}{\Delta\rho g} + \frac{14.72\sigma(\mu^D)^{0.4}(\mu^C)^{0.2}{d_h}^{-1.4}}{\Delta\rho g} \qquad (3.26)$$

The Reynolds number here is defined by

$$Re = \frac{d_h U_0 \rho^D}{\mu^D} \tag{3.27}$$

(4) Drop diameter is estimated from (Kumar and Hartland, 1982)

$$\frac{d_p}{d_h} = 1.591\left(\frac{\Delta\rho d_h U_0^2}{\sigma}\right)^{-0.068}\left(\frac{\Delta\rho d_h^2 g}{\sigma g_c}\right)^{-0.278} \qquad We < 2 \tag{3.28}$$

$$\frac{d_p}{d_h} = 1.546\left(\frac{\Delta\rho d_h U_0^2}{\sigma}\right)^{-0.021}\left(\frac{\Delta\rho d_h^2 g}{\sigma g_c}\right)^{-0.214} \qquad We > 2 \tag{3.29}$$

Thus, there are no parameters in the model that can be adjusted to fit the experimental data except the reference surface tension σ_{ref}. It seems that the predicted results are not sensitive to the value of σ_{ref}. When we varies its value from 25 to 35 (dynes per centimeter) the predicted results did not change much. In our simulations σ_{ref} is given the same value as used by Rocha and Fair, 35 dynes per centimeter.

3.6.1 Simulations

We have used the model described above to simulate the liquid-liquid extraction process in sieve tray columns for four multicomponent systems. Geometric details of the columns and operating conditions are summarized in Tables 3.1 and 3.2.

We used the mass transfer coefficient correlations of Rocha and Fair (1986). In our simulations, we consider the mass transfer contributions in the drop formation (or jetting) zone and drop rise/fall zone, and ignore the contributions from the coalescence zone.

The UNIQUAC equation for activity coefficients was used for estimation of the K-values and for the computation of the matrix of thermodynamic factor [Γ]. Interaction parameters were taken from the compilation by Sørensen and Arlt (1979).

Table 3.1: Data Sources for Four Systems in the Sieve Tray Columns.

Systems	U^D cm/s	U^C cm/s	$D_{col.}$ cm	Number of Trays	H_t cm	D_{hole} cm	Number of Holes	Ref.
M.I.B.K.-	0.63-	0.29-	10	10	16	.32	54	Rocha
Acetic Acid-	1.11	0.75		5	32	.32, .48	54, 21	& Fair
Water						.63	13	(1984)
Toluene-	0.55-	0.29-	10	10	16	.24, .32	123, 54	Rocha
						.48	33	& Fair
Acetone-	1.04	0.41		5	32	.32	54, 33	(1984)
Water				3	51	.32	54	
Toluene-			10.2	8	15.2	0.32	59	Garner
Diethyl								et al.
Amine-								(1953)
Water								
Diethyl			21.9	5	11.7	0.16	Free Area	Pyle
Ether-								et al.
Acetic Acid-						0.28	1.77-	(1950)
Water						0.51	5.05%	

The availability of these parameters was one of the criteria used in selecting sets of experimental data to simulate.

Typical specifications and simulation results for one experiment are shown in Table 3.3. More comprehensive comparisons between model prediction and experimental measurement are provided in Figures 3.3 to 3.7. Rocha (1984) and Garner et al. (1953) provided concentrations of the solute only; the solute concentrations are compared in Figures 3.3-3.5. In Pyle's (1950) paper, concentration measurements for all species are presented in the extract phase, but only solute concentration in the water phase. There is a total of forty four experiments listed in their paper. The results of our simulations for these experiments are shown in Figures 3.6 and 3.7. It is clear from Figures 3.6-3.7 that there is particularly good agreement with the experimental data for the extract liquid phase.

The standard deviations between the experimental data and simulation results are tabulated in Table 3.4. The standard deviations for the first three systems listed in Table 3.4 were less than 1%. The standard deviation for Pyle's data was about 2%.

Some simplifications of the rate equations have also been tested by simulation (primarily because the full model is rather demanding of computer time). These simplified models are:

1. Ignoring the matrix of thermodynamic factors $[\Gamma]$ (simplified model I in Table 3.5). More precisely, setting $[\Gamma] = [I]$, the identity matrix. Strictly speaking, this can only be true for an ideal liquid system for which no separation is possible (K-values would be unity). Nevertheless, even for nonideal fluids approximating $[\Gamma] = [I]$ is often possible.

2. Ignoring the matrix of flux correction factors, $[\Theta]$, (simplified model II in Table

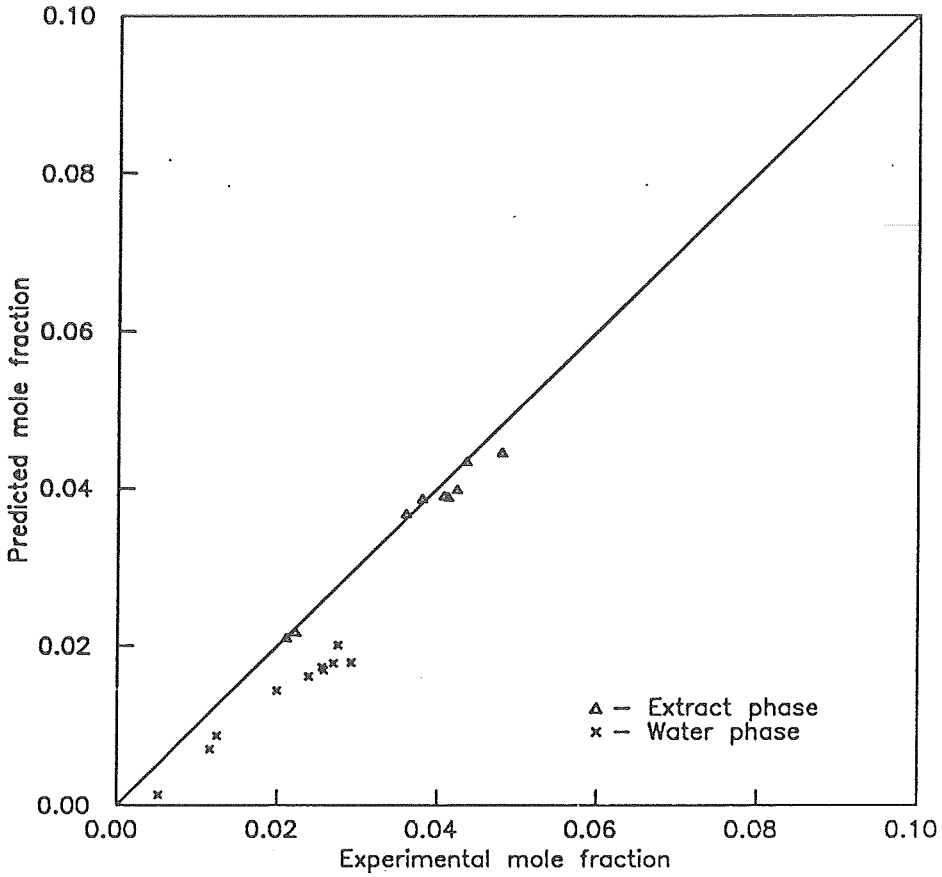

Figure 3.3: Concentrations of acetic acid in extract and water phases (experimental data from Rocha, 1984).

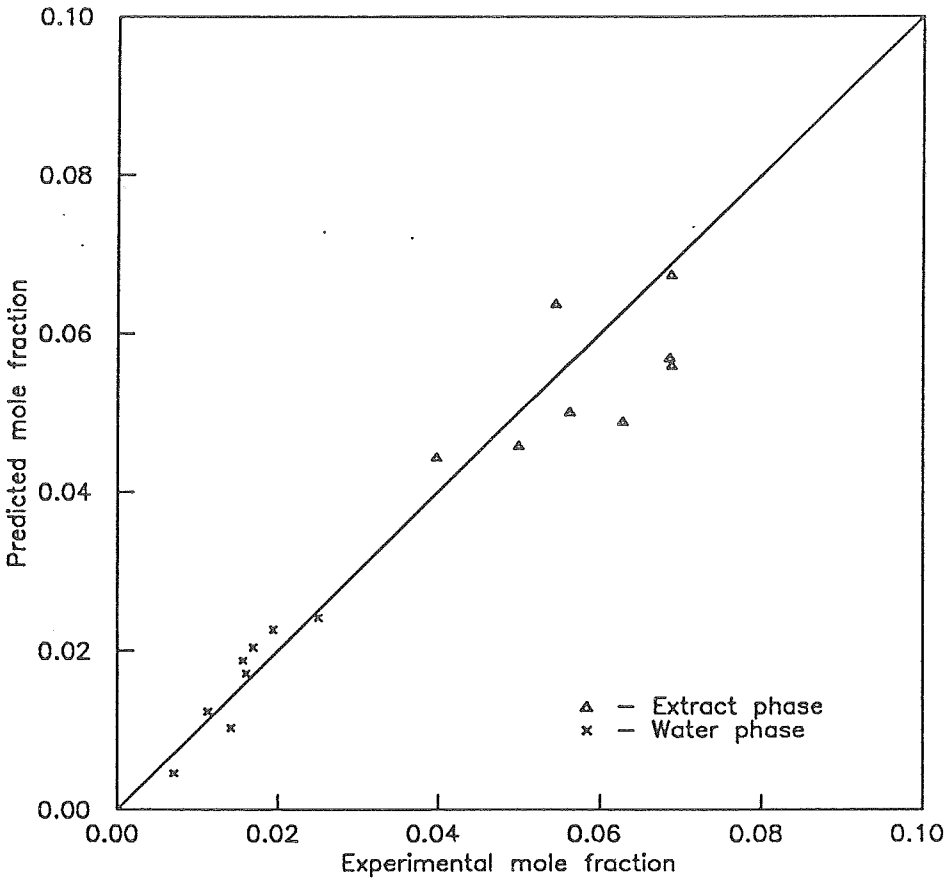

Figure 3.4: Concentrations of acetone in extract and water phases (experimental data from Rocha, 1984).

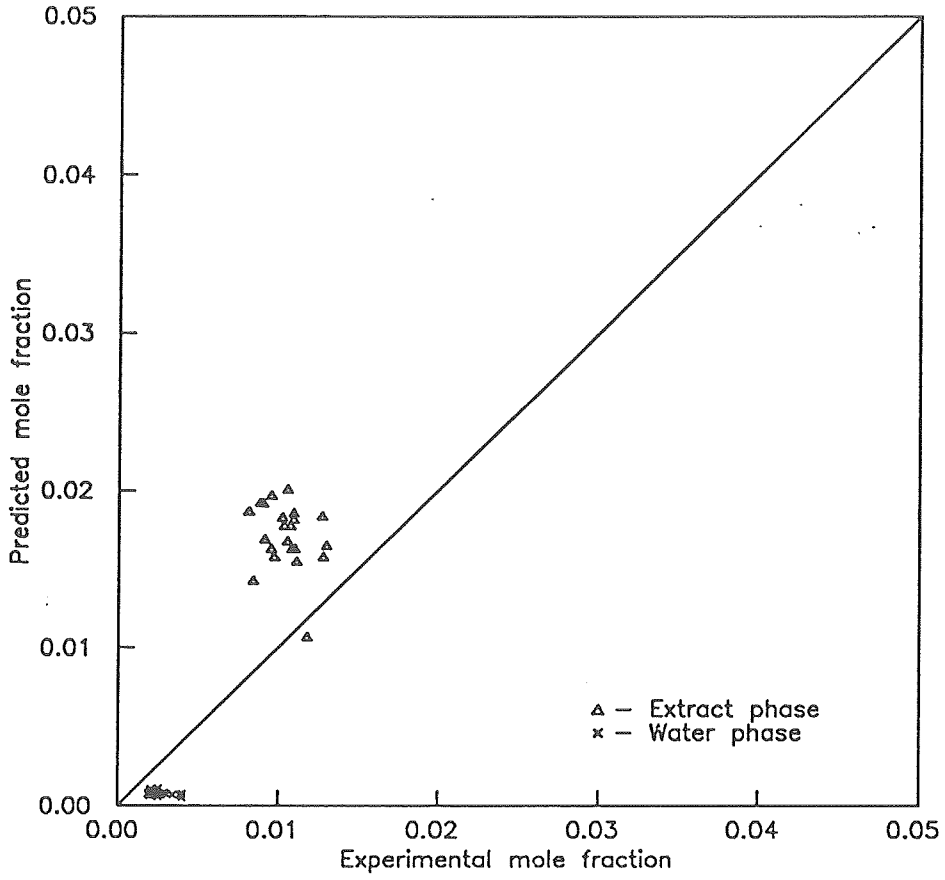

Figure 3.5: Concentrations of diethylamine in extract and water phases (experimental from Garner, 1953).

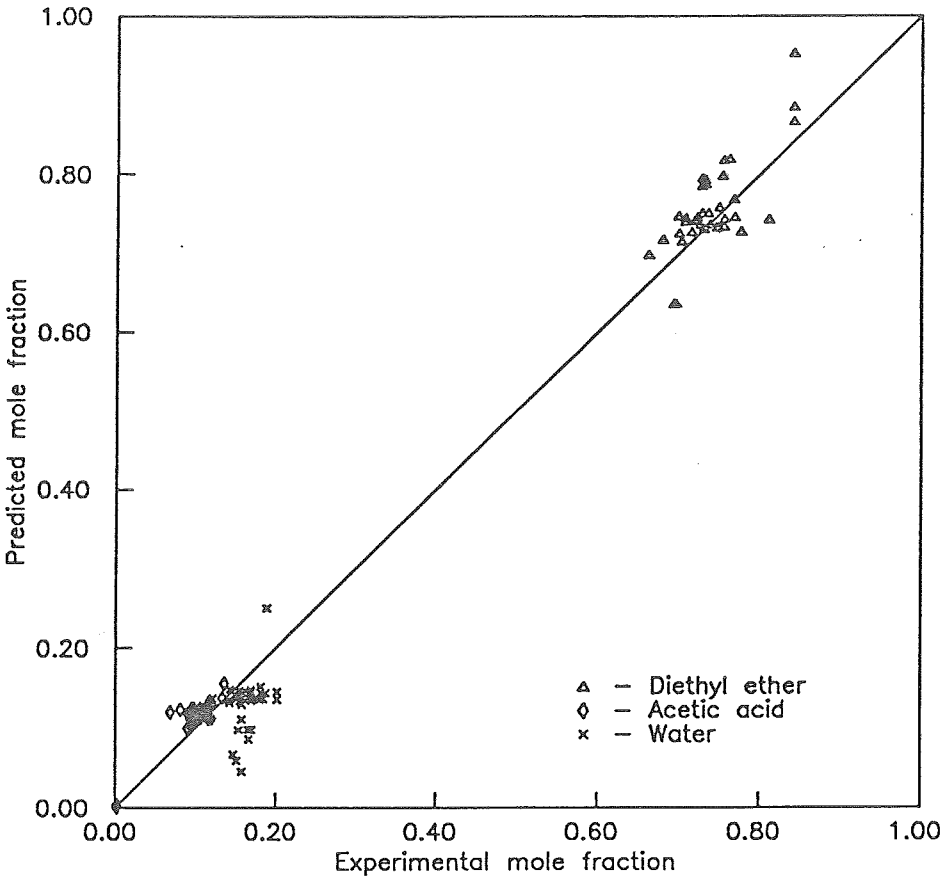

Figure 3.6: Comparison of predicted and experimental data (Pyle et al., 1950) in extract phase.

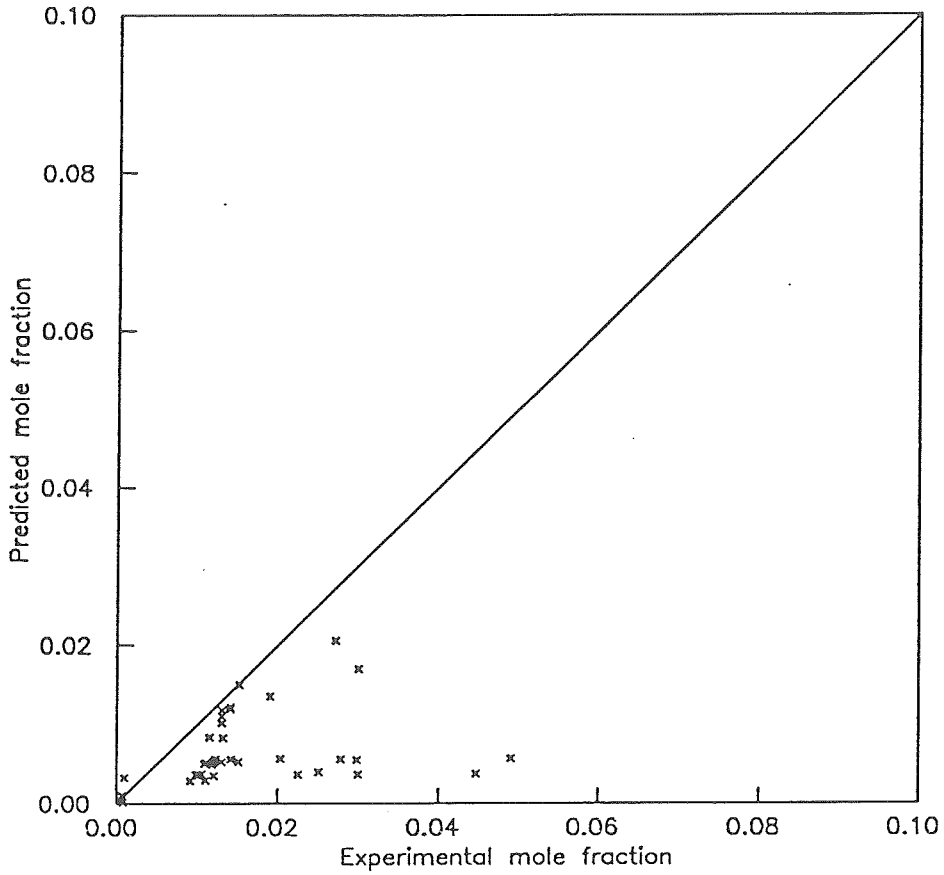

Figure 3.7: Concentrations of acetic acid in water phase (experimental data from Pyle et al., 1950).

3.5). In the limit of low rates of mass transfer $[\Theta] = [I]$. Mass transfer rates in extraction are not often very high so this should be a reasonable approximation anyway.

3. Ignoring both $[\Gamma]$ and $[\Theta]$ (simplified model III in Table 3.5), and computing $[k^*]$ simply as $[R]^{-1}$ (see Equation 3.8).

We used these three simplified methods to simulate the MIBK/acetic acid/water system of Rocha (1984). The composition profiles of two runs, numbers 35 and 39, are shown in Figures 3.8 and 3.9, respectively. The standard deviations for the complete solution model and the three simplified methods are included in Table 3.5. From these figures it can be seen that the three simplified methods have an accuracy comparable to that of the complete solution model and could be used with no significant loss of precision while reducing the computational cost of a simulation. It is likely that the uncertainties in the prediction of the mass transfer coefficients (and K-values) are too great to permit us to discriminate between the various models.

Krishna et al. (1989) recently presented the comments concerning Rocha (1986) model for mass transfer efficiency in sieve tray extractors. It is said that the Rocha's correlations overestimated the contribution of overall mass-transfer coefficient due to drop formation zone for systems with low interfacial tension, and gave a lower value of the column efficiency for drop rise zone. In our simulation the results showed a good agreement between the measurement and prediction. It is possible that the effects on overestimation for the drop formation zone and underestimation for the drop rise zone may eliminate each other, so that the deviation is reduced.

Other factors which affected the simulation results were also studied: sensitivity to the UNIQUAC interaction parameters, drop diameter and drop rise (or fall) velocity. We found that the predicted simulation results were most sensitive to the

UNIQUAC interaction parameters. The drop diameter and drop rise (or fall) velocity did not have significant effect on the predicted results. The moral here is that accurate liquid-liquid equilibrium models are of crucial importance even in a model of extraction based on the fundamentals of multicomponent mass transfer.

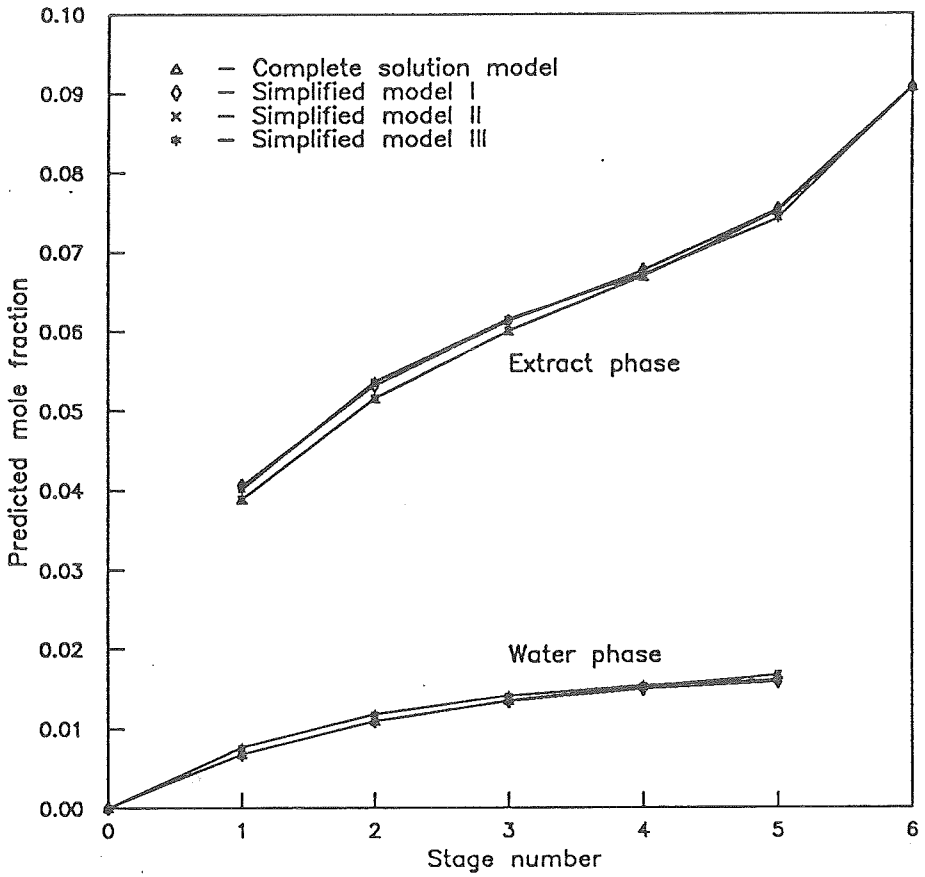

Figure 3.8: Composition profiles of acetic acid in extract and water phases in Run 35 of Rocha (1984).

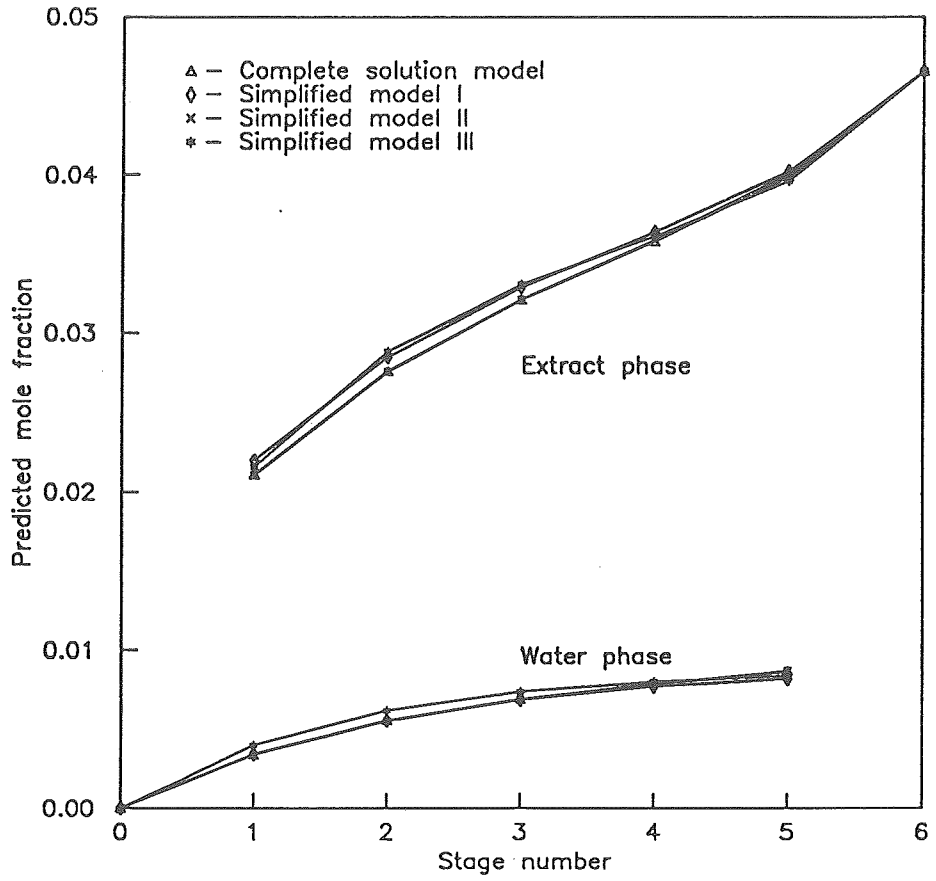

Figure 3.9: Composition profiles of acetic acid in extract and water phases in Run 39 of Rocha (1984).

Table 3.2: Plate Specifications in Pyle's Column (1950).

Plate *No.*	D_{hole}	Free Area
	cm	%
1	0.161	3.50
2	0.511	3.39
3	0.279	5.05
4	0.279	1.77
5	0.279	3.34

The plate number is counted consecutively from the top of the column to the bottom.

Table 3.3: Typical Specifications and Results for Diethylether - Acetic Acid - Water System (Pyle et al., 1950).

Stage Number		5
Column Diameter	cm	21.9
Tray Spacing	cm	11.7
Downcomer Diameter	cm	3.81

	Feed Flow Rate $kmol/s$		Feed Compositions $mol.\%$	
	Acid Phase	Ether Phase	Acid Phase	Ether Phase
Diethylether	0.1330×10^{-3}	2.2224×10^{-3}	3.36	95.17
Acetic Acid	0.3948×10^{-3}	0.78×10^{-6}	9.96	0.03
Water	3.4363×10^{-3}	0.1120×10^{-3}	86.68	4.80

Compositions of Exit Phases ($mol.\%$)

	Water Phase		Ether Phase	
	Experiment	Simulation	Experiment	Simulation
Diethylether	/	/	73.00	73.12
Acetic Acid	0.98	0.37	10.86	12.18
Water	/	/	16.15	14.71

Table 3.4: Standard Deviation of Four Systems.

	No.	Extract Phase *mol.%*		Water Phase *mol.%*	Ref.
MIBK-Acetic Acid-Water	9	0.19		0.79	Rocha & Fair
Toluene-Acetone-Water	8	0.97		0.28	Rocha & Fair
Toluene-Diethylamine-Water	22	0.74		0.20	Garner (1953)
Diethylether-Acetic Acid-Water	44	Comp. 1	2.35	1.61	Pyle (1950)
	44	Comp. 2	1.81		
	44	Comp. 3	1.75		

Comp. 1 - Diethylether

Comp. 2 - Acetic Acid

Comp. 3 - Water

Table 3.5: Standard Deviation for Different Models (Pyle's data).

Different Models	Number of Data Set	Extract Phase *mol.%*		Water Phase *mol.%*
Complete	44	Comp. 1	2.35	/
Solution Model	44	Comp. 2	1.81	1.61
	44	Comp. 3	1.75	/
Simplified	44	Comp. 1	2.78	/
Method I	44	Comp. 2	1.62	1.56
	44	Comp. 3	1.59	/
Simplified	44	Comp. 1	2.29	/
Method II	44	Comp. 2	1.82	1.59
	44	Comp. 3	1.91	/
Simplified	44	Comp. 1	2.72	/
Method III	44	Comp. 2	1.60	1.52
	44	Comp. 3	1.58	/

Comp. 1 - Diethylether; Comp. 2 - Acetic Acid; Comp. 3 - Water.

3.7 Summary

A nonequilibrium model has been used to simulate a number of liquid-liquid extraction operations in sieve tray columns with good agreement between experimental data and simulation prediction. The model presented above imposes no limits on:

1. the number of components present in the mixture (that includes both transferring species and solvents),

2. the number of feeds and sidestream products (although the latter would normally be zero) and

3. the type of extraction column.

There is an implicit requirement in the equilibrium relations (3.13) that all species be present in both phases. Species found in only one phase can be handled in the same way that noncondensable gases are modelled in a nonequilibrium model of multicomponent condensation (Taylor et al., 1986).

In view of the recent publication by Seibert and Fair (1988), (as well as the fact that the nonequilibrium stage model has been found equally useful for simulating trayed and packed distillation and absorption columns) the method described here should be useful for simulating packed extraction columns as well. Supercritical extraction is another possible application (see, for example, Lahiere and Fair, 1987).

Chapter 4

Nonequilibrium Models for Three Phase Distillation

4.1 General Model

A schematic diagram of a nonequilibrium stage for three phase distillation is shown in Figure 4.1. To formulate the equations of a nonequilibrium stage model and to describe the processes taking place on this tray is relatively straightforward in principle (although sometimes a little confusing in practice).

4.1.1 Material Balances

Material balances are constructed for all three phases. The total and component material balances for vapor phase are:

$$\mathtt{M}_{tj}^{V} \equiv V_j - V_{j+1} - F_j^V + N_{tj}^{V'} a_j^{V'} + N_{tj}^{V''} a_j^{V''} = 0 \tag{4.1}$$

$$\mathtt{M}_{ij}^{V} \equiv V_j y_{ij} - V_{j+1} y_{i,j+1} - F_j^V z_{ij}^V + N_{ij}^{V'} a_j^{V'} + N_{ij}^{V''} a_j^{V''} = 0 \tag{4.2}$$

The material balances for liquid phase $'$ include a term for mass transfer from the vapor phase (the same term as in the above two equations but with the opposite sign) and a term for mass transfer between the two liquid phases:

$$\mathtt{M}_{tj}' \equiv L_j' - L_{j-1}' - F_j' - N_{tj}^{'V} a_j^{V'} + N_{tj}^{'-''} a_j^{'-''} = 0 \tag{4.3}$$

$$\mathtt{M}_{ij}' \equiv L_j' x_{ij}' - L_{j-1}' x_{i,j-1}' - F_j' z_{ij}' - N_{ij}^{'V} a_j^{V'} + N_{ij}^{'-''} a_j^{'-''} = 0 \tag{4.4}$$

To these equations we must add the material balances for the second liquid phase:

$$\mathtt{M}_{tj}'' \equiv L_j'' - L_{j-1}'' - F_j'' - N_{tj}^{''V} a_j^{V''} - N_{tj}^{''-'} a_j^{'-''} = 0 \tag{4.5}$$

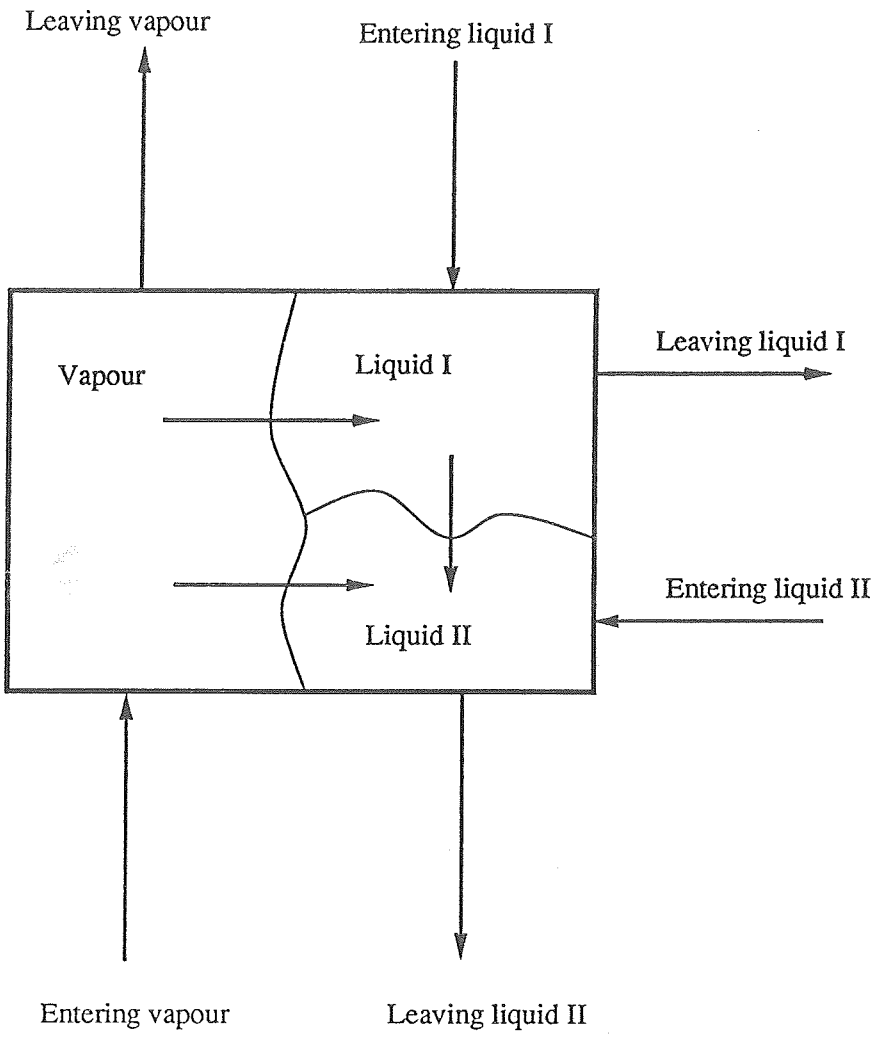

Figure 4.1: Schematic diagram of a nonequilibrium stage for three phase distillation.

$$M''_{ij} \equiv L''_j x''_{ij} - L''_{j-1} x''_{i,j-1} - F''_j z''_{ij} - N''^{V}_{ij} a^{V''}_j - N''^{-'}_{ij} a^{'-''}_j = 0 \qquad (4.6)$$

The material balance equations for the liquid phases could include additional terms representing the creation of liquid phase on a tray or disappearance of liquid phase from the tray. However, we know of no way to model this process and have treated this aspect of the problem in essentially the same way that it is handled in equilibrium stage models, by performing a liquid-liquid stability check on the liquid leaving a tray. If the liquid is unstable it is deemed to split into two phases and these two phases continue onto the next tray.

In the above equations N_{ij} are the molar fluxes, the double superscripted mass fluxes are the mass fluxes at the interface, the first superscript indicates the phase, the second the interface. For example, $N^{V'}_{ij}$ is the flux in the vapor phase at the vapor-liquid-$'$ interface, $N^{V''}_{ij}$ is the flux in the vapor phase at the vapor-liquid-$''$ interface, and $N^{'-''}_{ij}$ is the flux in liquid-$'$ at the liquid-$'$ and liquid-$''$ interface, $a^{V'}_j$ is the area of the vapor-liquid-$'$ interface, $a^{V''}_j$ is the area of the vapor-liquid-$''$ interface and $a^{'-''}_j$ is the area of the liquid-liquid interface. The single terms for the products of the fluxes and interfacial areas in Equations(4.1-4.6) will actually be a sum of terms representing mass transfer to bubbles or drops each with different character (size, velocity etc.).

The material balances for each phase are linked by the material balances around each interface :

- Material balance for the vapor - liquid phase-$'$ interface

$$N^{V'}_j - N^{'V}_j = 0 \qquad (4.7)$$

- Material balance for the vapor - liquid phase-$''$ interface

$$N_j^{V''} - N_j^{''V} = 0 \tag{4.8}$$

- Material balance for the liquid phase-$'$ - liquid phase-$''$ interface

$$N_j^{'-''} - N_j^{''-'} = 0 \tag{4.9}$$

As might be expected, the balance equations for all three phases and the interfaces can be added together to obtain Equation (1.20), the balance equations for the entire stage, the equations that are used in equilibrium stage simulation.

4.1.2 Energy Balances

In a nonequilibrium stage model of three phase distillation we need three energy balances as follows:

- Energy balance for the vapor phase

$$\mathrm{E}_j^V \equiv V_j \bar{H}_j^V - V_{j+1}\bar{H}_{j+1}^V + Q_j^V - F_j^V \bar{H}_j^{VF} + E_j^{V'} a_j^{V'} + E_j^{V''} a_j^{V''} = 0 \tag{4.10}$$

where Q_j^V is the heat exchanged with the environment,

- Energy balance for liquid phase-$'$

$$\mathrm{E}_j' \equiv L_j' \bar{H}_j' - L_{j-1}'\bar{H}_{j-1}' - Q_j' - F_j' \bar{H}_j^{'F} - E_j^{'V} a_j^{V'} + E_j^{'-''} a_j^{'-''} = 0 \tag{4.11}$$

- Energy balance for liquid phase-$''$

$$\mathrm{E}_j'' \equiv L_j'' \bar{H}_j'' - L_{j-1}''\bar{H}_{j-1}'' - Q_j'' - F_j'' \bar{H}_j^{''F} - E_j^{''V} a_j^{V''} - E_j^{''-'} a_j^{'-''} = 0 \tag{4.12}$$

$E_j^{V'}$, $E_j^{'V}$, $E_j^{V''}$, $E_j^{''V}$, $E_j^{'-''}$ and $E_j^{''-'}$ are the interfacial energy fluxes. As mentioned above the doubly superscripted energy fluxes are energy fluxes at the interface; the first superscript indicates the phase, the second the interface. For example, $E^{'-''}$ is the energy flux in the liquid-$'$ at the liquid-liquid interface, $E^{V'}$ is the energy flux in the vapor at the vapor-liquid-$'$ interface.

The energy fluxes in these equations are related by energy balances at each interface.

- Energy balance for the vapor-liquid phase-$'$ interface

According to the continuity of the energy flux across the interface

$$E_j^{V'} = E_j^{'V} \tag{4.13}$$

When the equation (2.9) is used for calculating the energy flux, the energy balance for the vapor-liquid interface becomes

$$\sum_{i=1}^{c} N_i^{V'} \lambda_i = 0 \tag{4.14}$$

where the λ_i are the enthalpy changes of vaporization.

Similarly,

- Energy balance for the vapor-liquid phase-$''$ interface

$$\sum_{i=1}^{c} N_i^{V''} \lambda_i = 0 \tag{4.15}$$

- Energy balance for the liquid-liquid interface

$$E_j^{'-''} - E_j^{''-'} = 0 \tag{4.16}$$

Mass transfer across the liquid-liquid interface is assumed equimolar because the partial enthalpies of components for two liquids can be regarded as the same, so that the liquid-liquid interfacial energy balance becomes

$$\sum_{i=1}^{c} N_i^{\prime-\prime} = 0 \tag{4.17}$$

4.1.3 Mass Transfer Rate Equations

We use the same rate equations mentioned in Chapter 2, but this time there are SIX sets of them, one for each side of each interface:

- Mass transfer from the vapor to the liquid-$'$ phase

$$(\mathrm{R}) \equiv [R^V]\left((N^{V'}) - N_t^{V'}(\bar{y})\right) - c_t^V(\bar{y} - y^{V'}) = (0) \tag{4.18}$$

$$(\mathrm{R}) \equiv [R']\left((N'^V) - N_t'^V(\bar{x}')\right) - c_t'[\Gamma'](x'^V - \bar{x}') = (0) \tag{4.19}$$

- Mass transfer from the vapor to the liquid-$''$ phase

$$(\mathrm{R}) \equiv [R^V]\left((N^{V''}) - N_t^{V''}(\bar{y})\right) - c_t^V(\bar{y} - y^{V''}) = (0) \tag{4.20}$$

$$(\mathrm{R}) \equiv [R'']\left((N''^V) - N_t''^V(\bar{x}'')\right) - c_t''[\Gamma''](x''^V - \bar{x}'') = (0) \tag{4.21}$$

- Mass transfer between the two liquid phases

$$(\mathrm{R}) \equiv [R']\left((N'^{-''}) - N_t'^{-''}(\bar{x}')\right) - c_t'[\Gamma'](\bar{x}' - x'^{-''}) = (0) \tag{4.22}$$

$$(\mathrm{R}) \equiv [R'']\left((N''^{-'}) - N_t''^{-'}(\bar{x}'')\right) - c_t''[\Gamma''](x''^{-'} - \bar{x}'') = (0) \tag{4.23}$$

The mole fractions identified with an overline represent the average composition in the bulk phase identified by the superscript. The double superscripted mole fractions are the compositions at the interface; the first superscript indicates the phase, the second the interface. For example, $x'^{-''}$ is the composition at the liquid-liquid interface in liquid phase $'$, $y^{V'}$ is the composition at the vapor-liquid-$'$ interface in vapor phase.

As we did in the two phase model (and for even stronger reasons), we assume that the interface compositions are the same at any point in the dispersion on the j-th tray.

4.1.4 Equilibrium at the Interface

The usual equations of phase equilibrium are used to relate the compositions at each interface:

- the vapor-liquid-$'$ interface:

$$\mathtt{Q}_{ij}^{V'} \equiv K'_{ij}\bar{x}_{ij}^{'V} - y_{ij}^{V'} = 0 \qquad i = 1, 2, \cdots c \qquad j = 1, 2, \cdots n \tag{4.24}$$

- the vapor-liquid-$''$ interface:

$$\mathtt{Q}_{ij}^{V''} \equiv K''_{ij}\bar{x}_{ij}^{''V} - y_{ij}^{V''} = 0 \qquad i = 1, 2, \cdots c; \qquad j = 1, 2, \cdots n \tag{4.25}$$

- the liquid-liquid interface

$$\mathtt{Q}_{ij}^{'-''} \equiv K^*_{ij}\bar{x}_{ij}^{''-'} - \bar{x}_{ij}^{'-''} = 0 \qquad i = 1, 2, \cdots c; \qquad j = 1, 2, \cdots n \tag{4.26}$$

The K-values are computed from appropriate models for the activity coefficients,

fugacity coefficients, vapor pressure and so on; they are computed using the compositions and temperature at the interface.

A very important difference between equilibrium and nonequilibrium models must be noted here. In the mass transfer model we do *not* solve a three phase equilibrium problem at the interface (or anywhere else for that matter) because we do not believe that all three phases in equilibrium exist together anywhere on a distillation tray. Only *two* phases come into contact at any particular time and place. This means that all three of Equations (4.24-4.26) are independent in the nonequilibrium model whereas only two of the three sets of the equilibrium relations (the Equations 1.21-1.23) are independent in the equilibrium model.

A consequence of this is that for the liquid-liquid equilibrium (LLE) computation we can use activity coefficient model parameters fitted to the LLE data whereas we can use parameters fitted to vapor-liquid equilibrium (VLE) data for the VLE calculations. We may even use two different sets of interaction parameters for the two independent VLE computations at the VL interfaces. Thus, the inability of existing thermodynamic models to fit three phase, vapor-liquid-liquid, equilibrium (VLLE) data as well as they fit two phase VLE and LLE data is much less critical in a mass transfer model than it would be in an equilibrium stage model. In fact, it may not even be desirable to use three phase VLLE data in fitting the parameters used in the interface equilibrium computations. Furthermore, we do not even have to use the same thermodynamic models for each interface if there is a good reason not to. For example, we might use UNIQUAC to model the vapor liquid equilibria and the NRTL equation to model the liquid-liquid equilibrium if that would provide better results. It should also be possible to use an activity coefficient model that does not admit two liquid phase (e.g. Wilson) in the VLE calculations.

4.1.5 Other Equations

The mathematical model is completed by equations that force the mole fractions of the bulk phases as well as the mole fractions at the interface to sum to unity (see Equations 1.3-1.4). Nine of these summation equations are needed.

4.1.6 Equations and Variables for a Single Nonequilibrium Stage

Given the state of all entering streams, the heat loads and pressures on the stage, there is a total of 15c+9 unknown variables and 15c+12 equations that permit the calculation of variable quantities for the j-th stage, which is shown in Table 4.1. However, the total material balances are not independent and the molar fluxes at the interface are equal to each other because of the continuity of the mass fluxes across the interface so the total number of independent variables or equations is $12c + 9$.

This completes the framework of a fairly general nonequilibrium model of three phase distillation. When we consider more detailed models we shall find that some of the equations presented above are dropped from the model while others are simplified. More on this topic below.

4.1.7 Relationship to Other Models

The general model described above reduces to the two phase model of Krishnamurthy and Taylor (1985a) if the second liquid phase is not present. If the vapor phase is not present then the model simplifies to the model of liquid-liquid extraction in Chapter 3.

Perhaps more interesting is the fact that the nonequilibrium model contains the equilibrium stage models of Chapter 1 as further limiting cases. Equilibrium between the bulk phases is attained when the driving forces (Δx) vanish. This will happen if the mass transfer coefficient interfacial area products are very high. In fact, if one

Table 4.1: Number of Variables and Equations of a Nonequilibrium Stage in Three Phase Distillation.

Variables	Number
The Vapor and Liquid Flows (V_j, L'_j, L''_j)	3
Vapour and Liquid Compositions (y_{ij}, x'_{ij}, x''_{ij})	$3c$
The Molar Fluxes	$6c$
The Interface Compositions	$6c$
The Vapor and Liquid Temperatures	3
The Interface Temperatures	3
Total	$15c + 9$

Equations	Number
Total Material Balances	3
Component Material Balances for each phase	$3c$
Component Material Balances for each interface	$3c$
Mass Transfer Rate Equations	$6(c-1)$
Interface Equilibrium	$3c$
Energy Balances	3
Interface Energy Balances	3
Bulk Mole Fraction Summations	3
Interface Mole Fraction Summations	6
Total	$15c + 12$

does a nonequilibrium simulation with interfacial areas about 100 times larger than they really are, then the results are very close to those obtained with an equilibrium model (Powers et al., 1988).

It is worth emphasizing that efficiency calculations are avoided completely in a nonequilibrium simulation. It is, however, possible to compute efficiencies from the results of a nonequilibrium simulation. In the equilibrium model, to obtain Murphree type efficiencies that are the same for all components on any given tray with just a single liquid phase requires all species to have the same facility for mass transfer. In addition, the resistance to mass transfer in the liquid phase must be totally negligible. If it is not, then the fact that the K-values are different for each component will ensure unequal point efficiencies. It is often claimed that distillation is a vapor phase controlled process (although this is not by any means a settled issue). However, the resistance to mass transfer in the liquid phase is probably higher in the kinds of systems likely to exhibit multiple liquid phases than it is in homogeneous systems. The higher liquid phase resistance would contribute to the much lower tray efficiencies that appear to be common in three phase distillation operations. Even if all of the foregoing were true, to have BOTH Murphree type efficiencies (Equations 1.29 and 1.30) the same requires, further, that the two liquid phases be in equilibrium with each other. This means that the liquid-liquid mass transfer coefficient interfacial area product must be very high. Mass transfer rates in liquid-liquid extraction are lower than those in vapor liquid distillation. So on the face of things it does not seem likely that the two Murphree efficiencies could possibly be equal. There is, however, some evidence that gas agitation of liquid-liquid extraction can increase mass transfer rates significantly (Priestly and Ellis, 1978). Herron et al. (1988) imply that this may be important in three phase distillation where vapor flow rates are 100 times or more the rates used by Priestly and Ellis.

4.2 Mass Transfer Coefficients and Interfacial Area

Since the use of empirical correlations for three phase distillation is of doubtful validity, we have begun to look at physically realistic mathematical models of the mass transfer character of a distillation tray. Recent work to this end is reported by, for example, Hofer (1983), Kaltenbacher (1982), Lockett et al. (1979), Prado and Fair (1987) and Lockett (1986). Krishna (1986) has used a model of this type to calculate efficiencies in multicomponent systems.

4.2.1 A Jet - Bubble Model

Kaltenbacher (1982) and Lockett and coworkers (1979, 1980 and 1983) have pictured the vapor passing through a liquid in cylindrical jets and spherical bubbles of varying sizes and velocities. Krishna (1985) and Krishna & Taylor (1986) have extended these models to multicomponent systems.

This Jet - Bubble model is used to describe the hydrodynamic and mass transfer behavior on a sieve tray. The flow pattern is shown in Figure 4.2. We may identify three mass transfer zones:

1. Zone I - Jetting/Bubble Formation Region

   Here the vapor issues through the perforations on the tray in the form of cylindrical jets, breaking into small and large bubbles. These jets could be modelled as a set of parallel cylindrical jets

2. Zone II - Free Bubbling Zone

   Just above the jetting/bubble formation zone is the free bubbling zone (bulk froth zone), where the vapor is dispersed in the form of rigid spherical bubbles of varying sizes through the froth and rise velocities, in Figure 4.2 represented by a bi-modal bubble size distribution: fast-rising "large" bubble and slow-rising

"small" bubble. The mass and heat transfer occurs in the dispersed bubbles and in the continuous phase (liquid).

3. Zone III - The Splash Zone

   Above the free bubbling zone, the vapor disengages from the liquid, small droplets are formed that are entrained in the vapor. This zone may be modelled as being made up of droplets of uniform size rising in plug flow through this region. But the contribution of the splash zone to the total mass transfer is generally negligibly small. In our simulation we ignored it.

The mass transfer coefficients in the zone I and the zone II are calculated respectively from equations (4.27-4.38)

In this jet-bubble zone model, Krishna (1985) suggested that for diffusion in the liquid phase the mass transfer coefficients be calculated from the penetration model solution for binary mass transfer given by

$$k^L = 2\sqrt{\frac{D}{\pi t}} \tag{4.27}$$

where k^L is the time-averaged binary mass transfer coefficient and t is the vapor-liquid contact time. For a multicomponent mixture the binary pair mass transfer coefficient k^L_{ij} is calculated by

$$k^L_{ij} = 2\sqrt{\frac{\mathcal{D}_{ij}}{\pi t}} \qquad i,j = 1,2,\cdots,c \tag{4.28}$$

where $\mathcal{D}_{ij}$ is the Maxwell-Stefan pair diffusivity.

For the dispersed gas/vapor phase, the mass transfer processes in the two zones I and II must be considered separately.

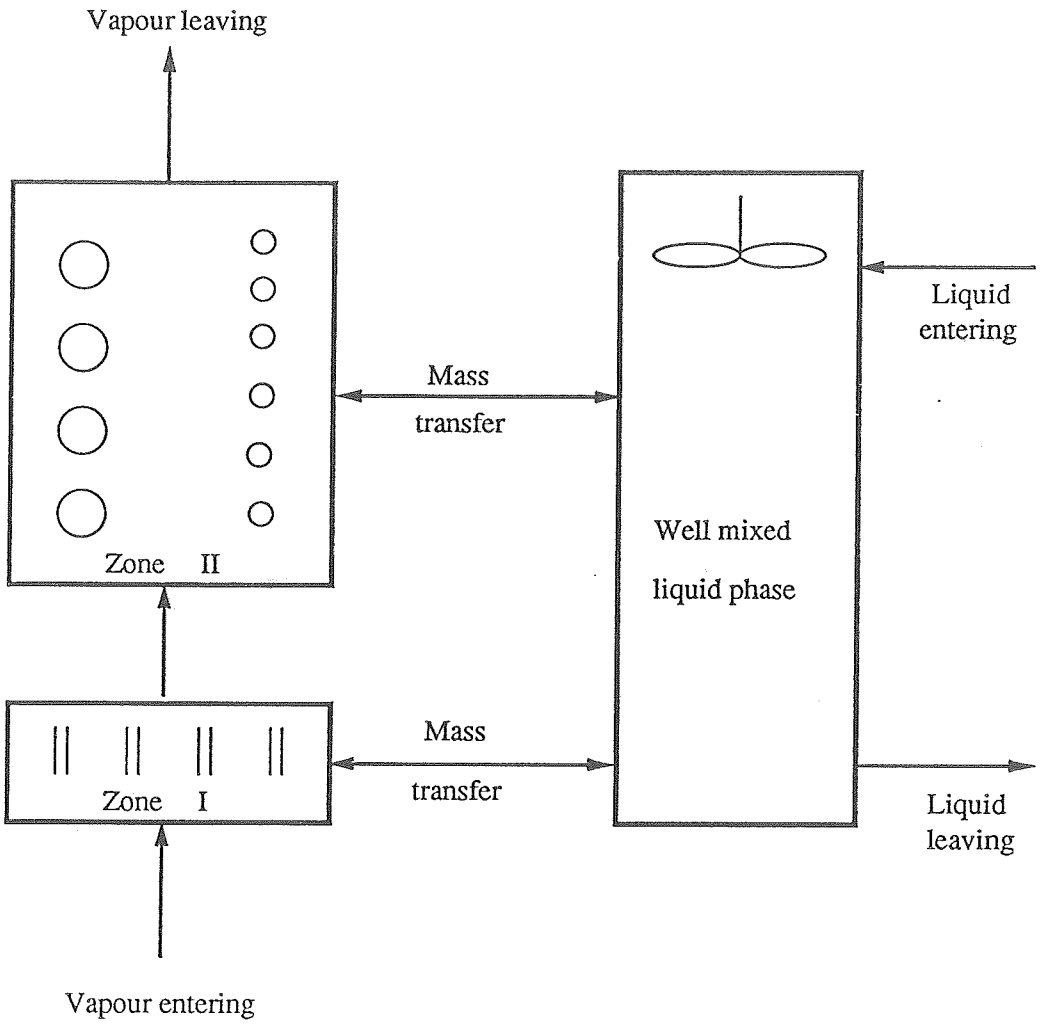

Figure 4.2: Flow pattern of jet-bubble model.

Formation zone

The time-average mass transfer coefficient k_{ij}^V is given by

$$k_{ij}^V = -\frac{1}{a'_I t_I} \ln \left(\sum_{m=1}^{\infty} \frac{4}{j_m^2} \exp\left(-Fo_I \frac{\mathcal{D}_{ij}}{\mathcal{D}_{ref}} j_m^2\right) \right) \tag{4.29}$$

where j_m is the roots of the Bessel function $J_o(j_m) = 0$. Fo_I is the Fourier number defined by

$$Fo_I = \frac{4\mathcal{D}_{ref} t_I}{d_I^2} \tag{4.30}$$

where d_I is the diameter of the cylindrical gas jet, the value chosen as same as the hole diameter. t_I is the gas residence time given by

$$t_I = \frac{h_I}{u_I} \tag{4.31}$$

where h_I is the height of the formation zone, the value chosen is about 5-10% of the froth height.

a' is the interfacial area per unit volume of dispersed gas given by

$$a'_I = \frac{4}{d_I} \tag{4.32}$$

u_I is the vapor velocity in the jet.

The gas velocity in the formation zone is related to the superficial velocity, u_s, by

$$u_s A_s = u_I a_h N_h \tag{4.33}$$

which can be used to estimate u_I as

$$\begin{aligned} u_I &= \frac{V}{c_t^V a_h N_h} \\ &= \frac{4V}{c_t^V \pi d_h^2 N_h} \end{aligned} \tag{4.34}$$

where u_s is the superficial velocity of vapor.

A_s is the across area of the column.

a_h is the hole area.

d_h is the diameter of holes.

N_h is the number of holes on the tray.

Bulk froth zone

In the bulk froth zone the following assumptions are made:

1. The bubble size has discrete population distribution.
2. Each population has uniform size bubbles.
3. The bubbles are assumed to be rigid spherical bodies.

The time-averaged mass transfer coefficient k_{ij}^V is given by

$$k_{ij_k}^V = -\frac{1}{a'_{II_k} t_{II_k}} \ln \left(\frac{6}{\pi^2} \sum_{m=1}^{\infty} \frac{1}{m^2} \exp\left(-\pi^2 m^2 Fo_{II_k} \frac{\mathcal{D}_{ij}}{\mathcal{D}_{ref}}\right) \right) \tag{4.35}$$

Subscript k represents the k-th population of bubbles. $\mathcal{D}_{ref}$ is the reference value of Maxwell-Stefan diffusivity, which is eliminated in the calculation.

The Fourier number is defined by

$$Fo_{II_k} = \frac{4\mathcal{D}_{ref} t_{II_k}}{d_{II_k}^2} \tag{4.36}$$

The gas residence time is calculated by

$$t_{II_k} = \frac{h_{II}}{u_{II_k}} \tag{4.37}$$

$$a'_{II_k} = \frac{6}{d_{II_k}} \tag{4.38}$$

The bubble size distribution and bubble rise velocities are determined by either experiment or correlation. Two distributions are available in the literatures (Ashley and Haselden, 1972; and Lockett et al., 1983). Two typical bubble size populations exist:

1. Small bubbles of 5 mm diameter with a rise velocity of 0.3 ms^{-1}, $f_k = 0.1$.

2. Large bubbles of about 12.5 mm diameter with a rise velocity calculated from continuity considerations (Lockett et al., 1983, 1986), $f_k = 0.9$.

3. h_{II} is the froth height h_f minus the small contribution of the formation zone. h_f can be measured or estimated from correlations (Fair, 1963; Mahendru et al., 1979 and Bennett et al., 1983).

Each zone contributes to the total interphase mass transfer. With the bulk and interface compositions assumed the same for all mass transfer zones, the driving forces ($\triangle x$, $\triangle y$) are the same for all zones and it is easy to derive the following relation for the total interphase mass transfer rates:

$$(N)a = c_t[\bar{R}]^{-1}a(\triangle y) + N_t a(\bar{y}) \quad , \tag{4.39}$$

where $[\bar{R}]^{-1}a$ is a matrix of mass transfer coefficients defined by

$$[\bar{R}]^{-1}a = [R_I]^{-1}a_I + \sum_k [R_{II_k}]^{-1}a_{II_k} \tag{4.40}$$

where the matrices $[R]$ on the right hand side represent the contributions due to the small bubble size, the large bubble size and the formation zone. The splash zone has been ignored in writing this expression, its contribution (here assumed negligible) could be incorporated simply by adding the appropriate term. A similar expression applies to the liquid phase.

4.3 Liquid Flow Models

Although the hydrodynamics of three phase distillation trays is still a subject for research, it seems reasonable, at least as a first step, to adopt the zone model of mass transfer described above to estimate the mass transfer coefficients and interfacial areas for a three phase distillation tray. The vapor is assumed to pass, either in the form of bubbles of a specified size or as cylindrical jets (or in a combination of both), through well mixed liquid phases. The multiplicity of liquid phases, however, means that we must say something about the way in which the liquids flow across the tray.

We propose four simple models of flow on three phase distillation trays:

1. The homogeneous liquid model
2. The segregated liquid model
3. The stratified liquid model and
4. The dispersed liquid model.

4.3.1 The Homogeneous Liquid Model

In this, the simplest possible model of a three phase tray, the two liquids are assumed to behave as a single homogeneous liquid. In principle, a correlation or

theoretical model developed for a two-phase dispersion could be used for the three-phase case by using the appropriate average physical properties and combined phase flow rates. An analogous approach was used by Grohse et al. (1949) and by Gerster et al. (1955) in their calculations of stage efficiency in the extractive distillation of C_4 hydrocarbons. The work of Herron et al. (1988) suggests that at least some three phase froth parameters (under some operating conditions) follow correlations developed for two phase dispersions.

The three phase nonequilibrium model simplifies to the two phase model presented above. This approach cannot be completely correct but it is the most reasonable starting point. The model will serve as the one against which all others will be judged.

4.3.2 The Segregated Liquid Model

In this model the vapor rises in plug flow through each liquid phase independently as though the two phases are separated on the tray by a longitudinal baffle (see Figure 4.3). Each liquid phase is assumed completely mixed.

If the two liquids remain completely segregated as they flow across a tray, there will be no liquid-liquid mass transfer and the liquid-liquid mass transfer rate and interfacial equilibrium relations are dropped from the model. If this model is valid then it does not seem very likely that the two liquids leaving a tray will be in equilibrium with other even if they were in equilibrium as they entered.

The flow rates of vapor passing through each liquid phase are calculated as follows

$$V'_{i,j+1} = (V_{i,j+1} + F^V_{ij})\frac{A'}{A_c} \tag{4.41}$$

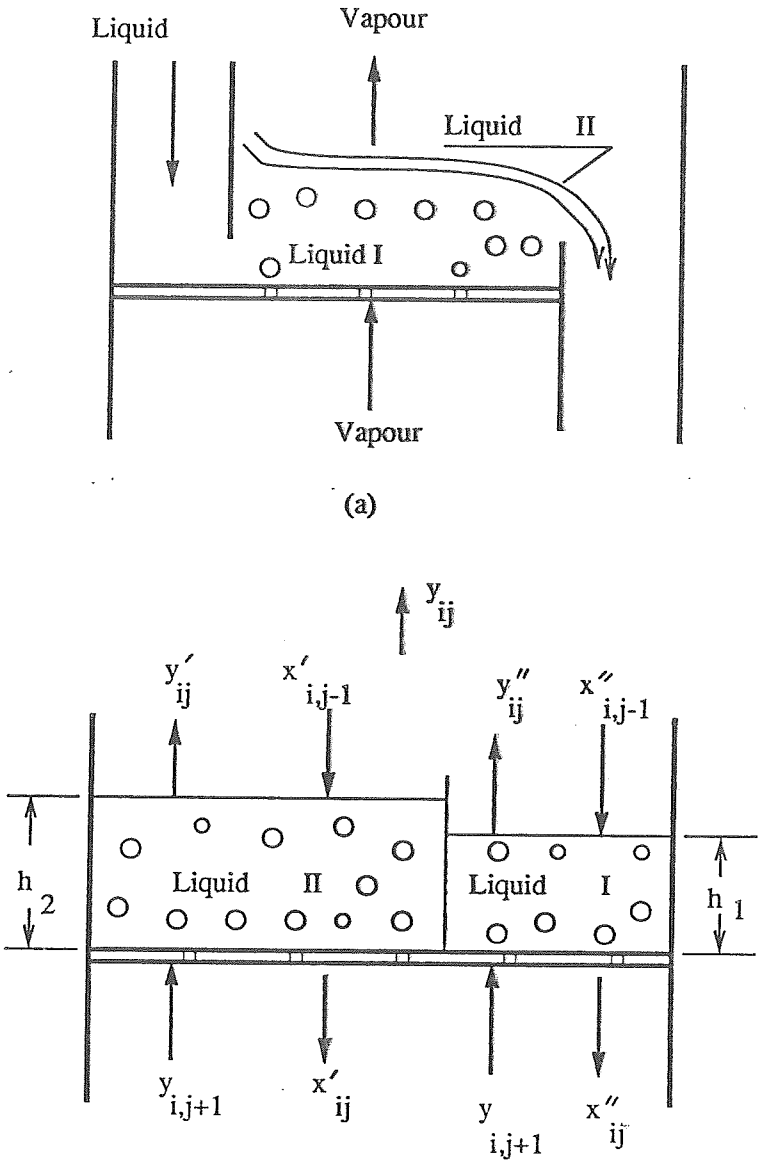

Figure 4.3: Schematic diagram of the segregated liquid model.

$$V''_{i,j+1} = (V_{i,j+1} + F^V_{ij})\frac{A''}{A_c} \tag{4.42}$$

where A' and A'' represent the tray area of each liquid phase which the vapor passes through, A_c is the total active area of the tray.

$$A' + A'' = A_c \tag{4.43}$$

We assume that the two liquid phases have the same hydrostatic pressure; thus, the vapor distribution on the tray would be nearly equal, i.e.

$$h'_l \rho' = h''_l \rho'' \tag{4.44}$$

where ρ is the liquid phase density, h_l is the equivalent height of the clear liquid.

$$\rho' = \bar{M}' c'_t \tag{4.45}$$

$$\rho'' = \bar{M}'' c''_t \tag{4.46}$$

where $\bar{M}$ is the average molecular weight.

From equations (4.44-4.46) we can calculate the height ratio of two liquid phases r_h.

$$r_h = \frac{h'_l}{h''_l} = \frac{\bar{M}'' c''_t}{\bar{M}' c'_t} \tag{4.47}$$

Since:

$$\frac{h'_l A'}{h''_l A''} = \frac{L'/c'_t}{L''/c''_t} \tag{4.48}$$

So that A' and A'' can be calculated from equations (4.43) and (4.49).

$$\begin{aligned} \frac{A'}{A''} &= \frac{c_t''}{c_t'}\frac{L'}{L''}\frac{h''}{h'} \\ &= \frac{c_t''}{c_t'}\frac{L'}{L''r_h} \end{aligned} \tag{4.49}$$

The total flow rate of leaving vapor is found from:

$$V_{ij} = V_{ij}' + V_{ij}'' \tag{4.50}$$

For two liquid phases, the flow rates can be calculated respectively from:

$$L_{ij}' = L_{i,j-1}' + F_{ij}' + N_{ij}'^{V} a_j^{V'} \tag{4.51}$$

$$L_{ij}'' = L_{i,j-1}'' + F_{ij}'' + N_{ij}''^{V} a_j^{V''} \tag{4.52}$$

The mass transfer fluxes in the interface between the vapor and each liquid phase can be determined with Equations (2.11 and 2.12).

This model is, however, the simplest three phase model that can take two liquid phases separately into account. The model is equivalent to two two-phase mass transfer models in parallel; after the homogeneous liquid model, it is the easiest to implement.

4.3.3 The Stratified Liquid Model

The third model is the *stratified liquid model* in which we assume that the vapor passes through each liquid phase in turn. There would not be much mass transfer between the two liquid phases in this model since the area available for liquid-liquid

transfer is negligible. This allows us to drop some of the model equations from the complete set of model equations and to simplify some of the others. The scheme of this model is shown in Figure 4.4. The component mass balances for each liquid phase are as follows

$$M'_{ij} \equiv L'_{ij}x'_{ij} - L'_{j-1}x'_{i,j-1} - F'_j z'_{ij} - N'^{V}_{ij} a^{V'}_j = 0 \tag{4.53}$$

$$M''_{ij} \equiv L''_{ij}x''_{ij} - L''_{j-1}x''_{i,j-1} - F''_j z''_{ij} - N''^{V}_{ij} a^{V''}_j = 0 \tag{4.54}$$

The total vapor molar flux is equal to the vapor molar flux in zone (I) plus the vapor molar flux in zone (II). For the vapor phase the component material balance is given by

$$M^V_{ij} \equiv V_j y_{ij} - V_{j+1} y_{i,j+1} - F^V_j z^V_{ij} + N^{V'}_{ij} a^{V'}_j + N^{V''}_{ij} a^{V''}_j = 0 \tag{4.55}$$

In this model we assume that the froth height ratio of two phases only depends on the ratio of the liquid volume of these phases, that means:

$$\frac{h'}{h''} = \frac{L'}{c'_t}\frac{c''_t}{L''} \tag{4.56}$$

and

$$h' + h'' = h \tag{4.57}$$

from the equations (4.56-4.57) the froth height of each liquid phase can be determined.

This model is not totally unreasonable when the vapor flow rate is small, two liquid phases may lie one above the other (see Ashton et at., 1987).

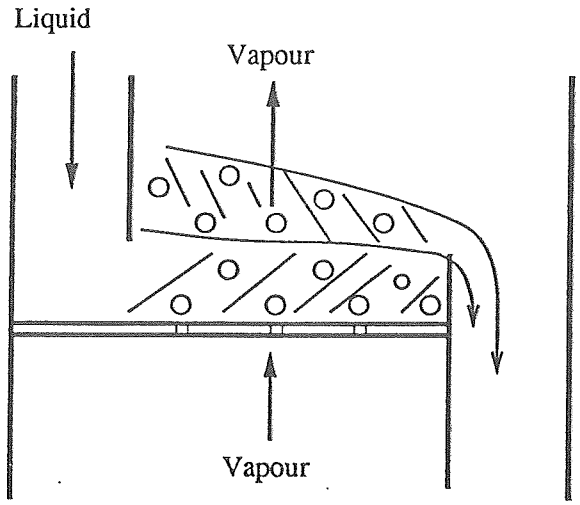

(a)

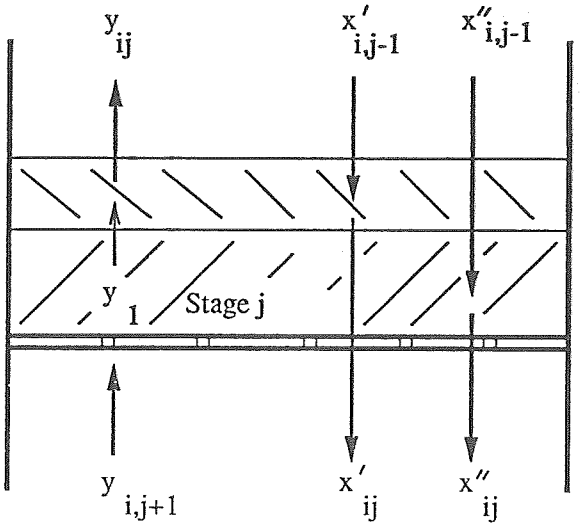

(b)

Figure 4.4: Schematic diagram of the stratified liquid model.

4.3.4 The Dispersed Liquid Model

Our fourth and last model is the most realistic of all but also the most difficult to implement since we now need to consider liquid-liquid mass transfer explicitly for the first time. This is the dispersed liquid model in which we assume that one liquid is dispersed completely in the other. Only the continuous liquid-"*sees*" the vapor phase. The schematic diagram is shown in Figure 4.5. For the vapor phase material balance, Equation (4.1) simplifies to

$$\mathtt{M}_{ij}^{V} \equiv V_j y_{ij} - F_j^V z_{ij}^V - V_{j+1} y_{i,j+1} + N_{ij}^{V''} a_j^{V''} = 0 \tag{4.58}$$

For the dispersed liquid phase, the material balance now reads

$$\mathtt{M}_{ij}^{'} \equiv L_j' x_{ij}' - F_j' z_{ij}' - L_{j-1}' x_{i,j-1}' + N_{ij}^{'-''} a_j^{'-''} = 0 \tag{4.59}$$

The material balance for the continuous liquid phase is given by Equation (4.60)

$$\mathtt{M}_{ij}^{''} \equiv L_j'' x_{ij}'' - F_j'' z_{ij}'' - L_{j-1}'' x_{i,j-1}'' - N_{ij}^{''V} a_j^{V''} - N_{ij}^{''-'} a_j^{'-''} = 0 \tag{4.60}$$

where the superscript $'$ represents the dispersed liquid phase and $''$ the continuous liquid phase, $N_{ij}^{V''}$ is the molar flux of vapor at the vapor-continuous liquid interface, and $N_{ij}^{'-''}$ is the flux of the dispersed liquid at the liquid-liquid interface.

The mass transfer flux between the dispersed liquid and the continuous liquid phases is estimated from a model similar to the model that determines the mass transfer flux in the bubble zone. Equations (4.35-4.38) can be used to calculate the time average mass transfer coefficients of the dispersed liquid phase. Two populations of drops are considered in this model. Equation (4.28) is used to determine the mass transfer coefficient of the continuous liquid phase.

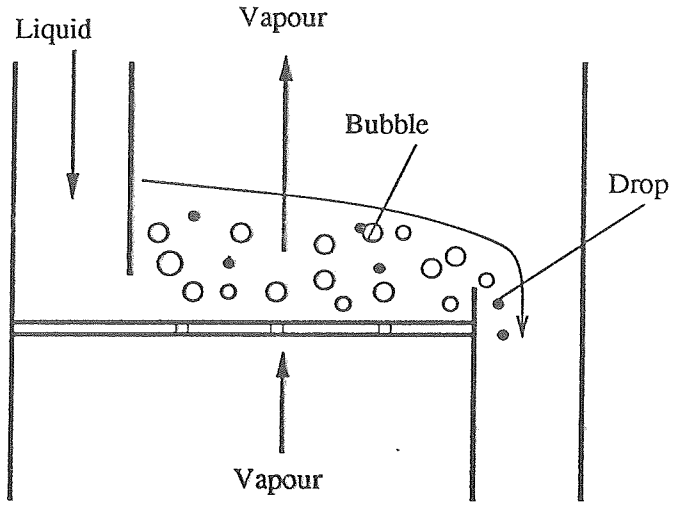

(a)

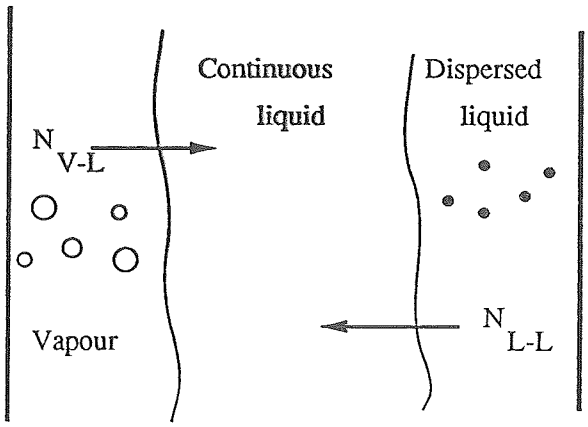

(b)

Figure 4.5: Schematic diagram of the dispersed liquid model.

4.4 Simulation Procedure for a Single Stage

In our previous work mentioned in Chapter 2 and Chapter 3, Newton's method is used to solve all the nonequilibrium model equations for all stages simultaneously. In an azeotropic distillation column, two or more than two liquid phases may coexist in some or all stages of the column. We do not know in advance where two liquid phases appear or disappear. It is better to focus on solving the model equations for a single tray.

The computation procedure shown in Figure 4.6 is applied in the simulation. The component flow rates of the vapor leaving the tray and one or two entering liquids, temperature and pressure for a given stage are specified. The first step is a judgement of how many liquid phases would coexist in that specified stage (see Section 4.4.1 below). If only one liquid phase is present, the homogeneous liquid model will be used for the further simulation; if two liquid phases coexist, one of the three heterogeneous liquid models, the segregated liquid model, the stratified liquid model or the dispersed liquid model, might be selected arbitrarily for the simulation. When the initial guesses of the interface temperature and flow rates of entering vapor and leaving liquid phases are given, the calculation of the mass transfer coefficients and fluxes may be carried out. The flow rates of the entering vapor and leaving liquid phases are determined from the material balances. Finally, a matrix norm defined in Equation (4.61) is used as the convergent criterion.

$$\sqrt{\sum_{i=1}^{c} \left(X_i^{k+1} - X_i^k\right)^2} < tolerance \tag{4.61}$$

The iterations continue until the results satisfy the equation (4.61).

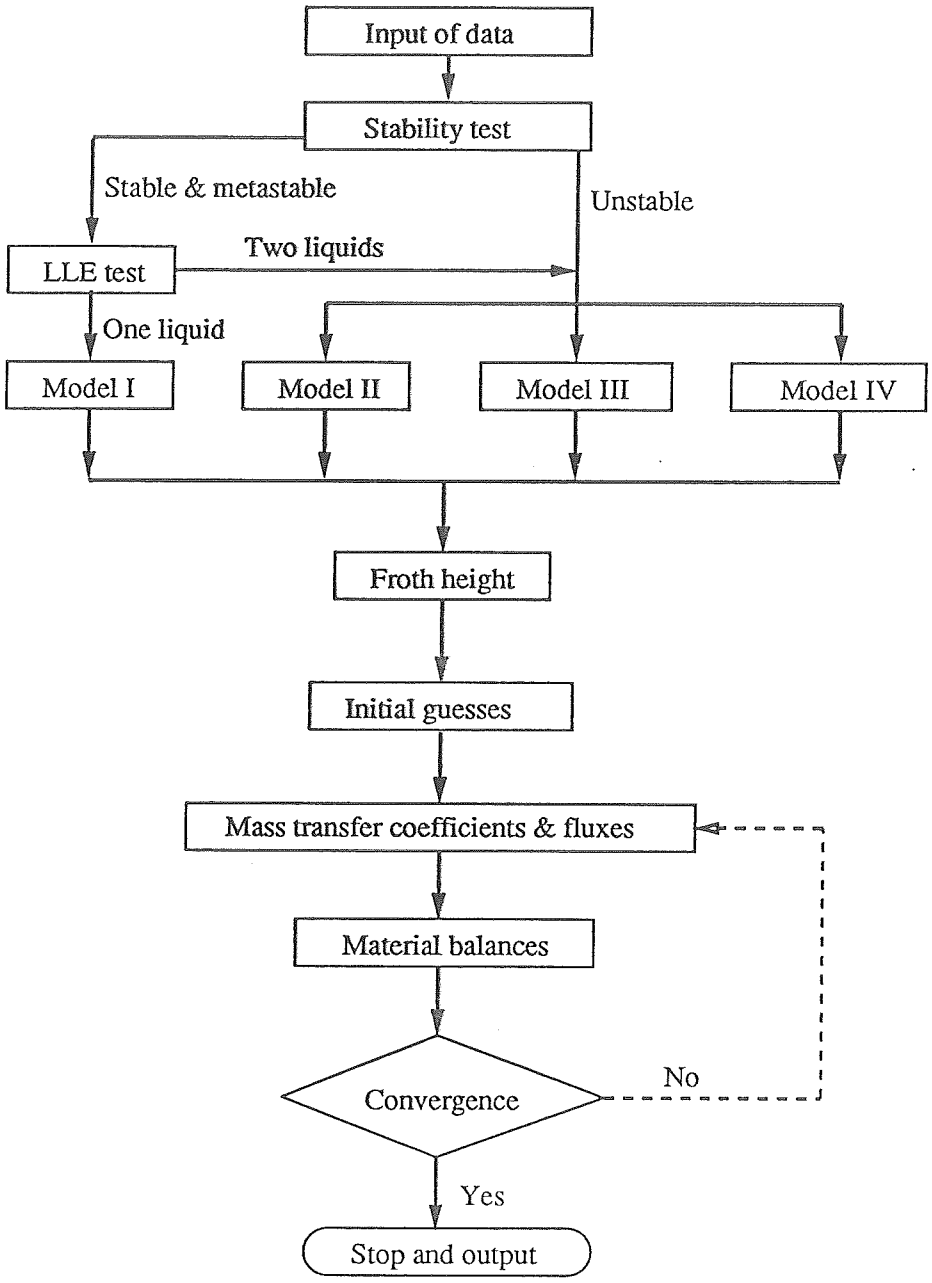

Figure 4.6: Computation procedure.

4.4.1 Stability Test of the Liquid Mixture

There has been considerable interest during the recent few years in thermodynamic stability tests. From phase splitting principles a mixture would be either stable or unstable. There is still one more possible state between these two states which is called meta-stable, sometimes called "locally stable" (see Appendix A). In the paper published by Van Dongen et al. (1983), only intrinsically unstable mixtures were considered unstable; meta-stable mixtures were treated as stable. They used a mathematical criterion of the positive semidefinite matrix $[\varrho]$ which represented the second derivative of molar Gibbs free energy to conclude that "the two phase azeotropic equilibrium might be stable if one of the phases is materially unstable providing the other phase is so strongly stable". Concerning this criterion of thermodynamic stability, it seems, there is some different comment. Michelsen (1984) mentioned that this conclusion of two phase azeotropic equilibrium was incorrect. Maurer and Prausnitz (1979) recognized that the positive determinant of the matrix $[\varrho]$ can not, without further calculation, determine whether one or two liquid phases coexist.

In our simulations we consider a meta-stable mixture leads to two liquid phases, because vapor and liquid phases on the tray contact in turbulent flow. We use the positive definiteness of the Hessian matrix of the Gibbs free energy as the initial criterion of thermodynamic stability. If any eigenvalue of the Hessian matrix is negative, two liquid phases will coexist. But if all the eigenvalues are positive, a further test of whether or not two liquid phases present must be carried out. The calculation for this purpose is a liquid-liquid equilibrium computation. If the compositions of two liquid phases obtained from liquid-liquid equilibrium calculation are the same, it means that only one liquid phase is present.

It is noted that the convergence of liquid-liquid equilibrium calculation is much more sensitive to the initial guess than those for vapor-liquid equilibrium. Vari-

ous initialization schemes were presented by Prausnitz (1980), and Ohanomah and Thompson (1984). The procedure used for initialization in this study, adopted from the latter work, is summarized in Table 4.2.

This procedure has been tested for several systems (data are from Prausnitz, 1980; Block and Hegner, 1976 and Walraven et al. 1988) summarized in Table 4.3.

4.4.2 Calculation of the Fluxes

For solving the nonequilibrium model, the key procedure is the calculation of mass transfer fluxes. The jet-bubble model mentioned in Section 4.3 and the similar drop model are used for calculating mass transfer coefficients and fluxes in the vapor and each liquid phase.

The molar diffusion fluxes are calculated from Equation (2.12) as

$$\begin{aligned}(J) &= c_t^V[\bar{R}^{OV}]^{-1}\Delta\bar{y} \\ &= c_t^V[\bar{R}^{OV}]^{-1}(\bar{y}-\bar{y}*) \end{aligned} \tag{4.62}$$

where $\bar{y}*$ is the composition of a vapor in equilibrium with the bulk liquid phase, $\Delta\bar{y}$ is the driving force of mass transfer.

$[\bar{R}^{OV}]$ is an overall matrix of inverted mass transfer coefficients defined by Equation (4.63) (see Appendix B and Krishna, 1985).

$$[\bar{R}^{OV}] = [\bar{R}^V] + \frac{c_t^V}{c_t^L}[K^{eq}][\bar{R}^l][\bar{\beta}^l]^{-1}[\bar{\beta}^V] \tag{4.63}$$

where $[\beta]$ is a bootstrap matrix with elements

$$\beta_{ij} = \delta_{ij} - x_i\left[\frac{\lambda_i - \lambda_c}{\sum_{i=1}^{c} x_i\lambda_i}\right] \qquad i,j = 1,2,\cdots,c-1 \tag{4.64}$$

Table 4.2: An Initialization Procedure for Liquid-Liquid Equilibrium.

1. Set $x' = z$ and calculate γ'.

2. Set $x'' = z^T\gamma'$.

3. Normalize x'' and estimate γ''.

4. Compute $K = \gamma'/\gamma''$.

5. Define K_{IE} as the largest K_i and K_{IR} the smallest K_i for all species i.

6. Assume $x'(R) = x''(E) = 0.98$ and $x'(E) = X''(R) = 0.02$.

7. Initialize K.

8. Initialize liquid phase fraction $\alpha'^0 = L'/F$ from

$$\alpha'^0 = \frac{z_E(1 - 1/K_{IE}) + K_{IR}z_R}{z_E + z_R}$$

9. Calculate the moles of the given components from:

$$L''^0_i = \frac{z_i}{1 + \frac{1-\alpha'^0}{\alpha'^0}K'_i}$$

10. Determine the liquid phase fraction, α, and compositions from material balances.

11. Iteration procedure: If $\alpha > 1$ go to Step 3; if $0 < \alpha < .1$, stop and output the initial values of compositions of two liquid phases.

Table 4.3: Results of Liquid Phase Splitting Tests.

System	Number of Tests	Maximum Deviation *mol.%*	Number of Fail* Tests	Reference
Furfural-Benzene-2,2,4-Trimethylpentane	2	< 0.01	0	Prausnitz et al., 1980
Furfural-2,2,4-Trimethylpentane-Cyclohexane	2	< 0.01	0	As Above
Water-Acrylonitrile-Acetonitrile	2	< 0.01	0	As Above
Furfural-2,2,4-Trimethylpentane-Pentane-Cyclohexane	3	< 0.01	0	As Above
Water-n-Butanol-n-Propanol	9	< 0.01	2	Walraven et al., 1988
Water-n-Butanol-n-Propanol	12	< 0.01	2	Block et al., 1976

*fail means opposite results vs. in Reference such as, no phase splitting vs. phase splitting in Reference or vice versa.

used to describe the non-equimolar transfer character. δ_{ij} is the Kronecker delta. For equimolar transfer $[\beta] = [I]$.

The average driving force is estimated from

$$\Delta y = \frac{\Delta y_E + \Delta y_L}{2} \tag{4.65}$$

where $\Delta y_E = (y - y*)_E$ and $\Delta y_L = (y - y*)_L$, and subscripts E and L represent the entering and leaving streams respectively. The driving forces, Δy_E and Δy_L, are related by (Krishna, 1985)

$$\Delta y_L = [Q]\Delta y_E \tag{4.66}$$

For the jet-bubble model, the matrix $[Q]$ is given by Krishna (1985) as

$$[Q_{jet}] = \exp\left[[-\bar{R}^{OV}_{jet}]^{-1} a'_{jet} t_{jet}\right] \tag{4.67}$$

$$[Q_{bub_k}] = \exp\left[[-\bar{R}^{OV}_{bub_k}]^{-1} a''_{bub_k} t_{bub_k}\right] \tag{4.68}$$

$$[Q_{bub}] = \sum_{k=1} f_k [Q_{bub_k}] \tag{4.69}$$

Equations (4.66-4.69) can be derived assuming the vapor rises in plug flow through the liquid.

4.5 Applications, Results and Discussion

There is a marked shortage of good data that is suitable for testing the three phase nonequilibrium model. The most complete set of data is that recently published by Cairns and Furzer (1987a). Our simulations are based on their experimental data.

Ethanol dehydration experiments were carried out in a glass column with nine sieve trays without downcomer, column diameter is 104 mm, which operates at total reflux. The geometric parameters of the column are listed in Table 4.4.

The dehydration agent consists of a total of ten hydrocarbons. The major components are trimethylpentane isomers. In order to simulate their experiments we simplify the system to a ternary system: ethanol - water - 2,2,4-trimethylpentane. The amount of the other hydrocarbons is quite small compared with the amount of 2,2,4-trimethylpentane.

4.5.1 Simulation Results

There are four sets of experimental data published in Cairns and Furzer (1987a) paper. Two sets of data, Run 7 and Run 8, showed that only one liquid phase on all stages of the column; the other two sets, Run 1 and Run 2, indicate that two liquid phases coexist on all stages. We used the routines to test how many liquid phases coexisting on the given stage, the predicted number of liquid phases is consistent with the experimental data.

We compare the simulation results with the measured mole fractions for Run 7 and Run 8 (Cairns and Furzer, 1987), which are shown in Figures 4.7 and 4.8. It is obvious that the homogeneous liquid model (Model I marked in the figures), in which mass transfer coefficients and fluxes are determined based on a theoretical model, is reasonable and reliable for simulation of two phase distillation. The specifications of one set of data and comparison between the predicted and measured compositions are listed in Tables 4.5 and 4.6, respectively, for Run 7 and Run 8.

The comparison for Run 1 and Run 2 are shown in Figures 4.9 to 4.14, which present the results obtained from the segregated liquid model (marked Model II), the stratified liquid model (Model III) and the dispersed liquid model (Model IV).

Table 4.4: Geometric Parameters of the Column (Cairns and Furzer, 1987a).

Column Diameter	m	0.104
Number of Trays		9
Spacing	m	0.32
Type of Trays		Sieve Tray Without Downcomer
Hole Diameter	m	0.008
Number of Holes		34
Free Area	%	0.201

Table 4.5: Specifications and Results of Stage 3 (Run 7, Cairns and Furzer, 1987a).

Component	Feed Flow Rate $(kmol/s)$
Ethanol	$0.1514 \times (10)^{-3}$
Water	$0.1398 \times (10)^{-4}$
Hydrocarbons	$0.6586 \times (10)^{-4}$

Component	Compositions $(mole\ fraction)$	
	Experiment	Simulation
Ethanol	0.6998	0.6542
Water	0.0435	0.0593
Hydrocarbons	0.2567	0.2865

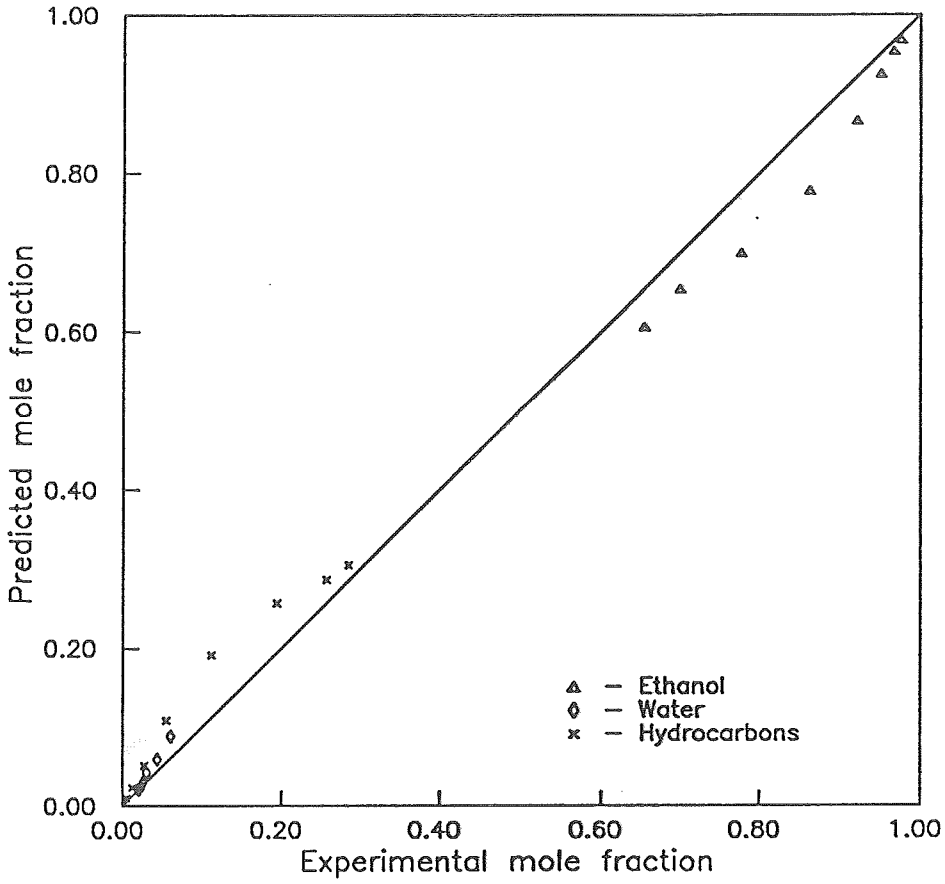

Figure 4.7: Comparison of predicted and experimental compositions (Run 7, Cairns and Furzer, 1987a).

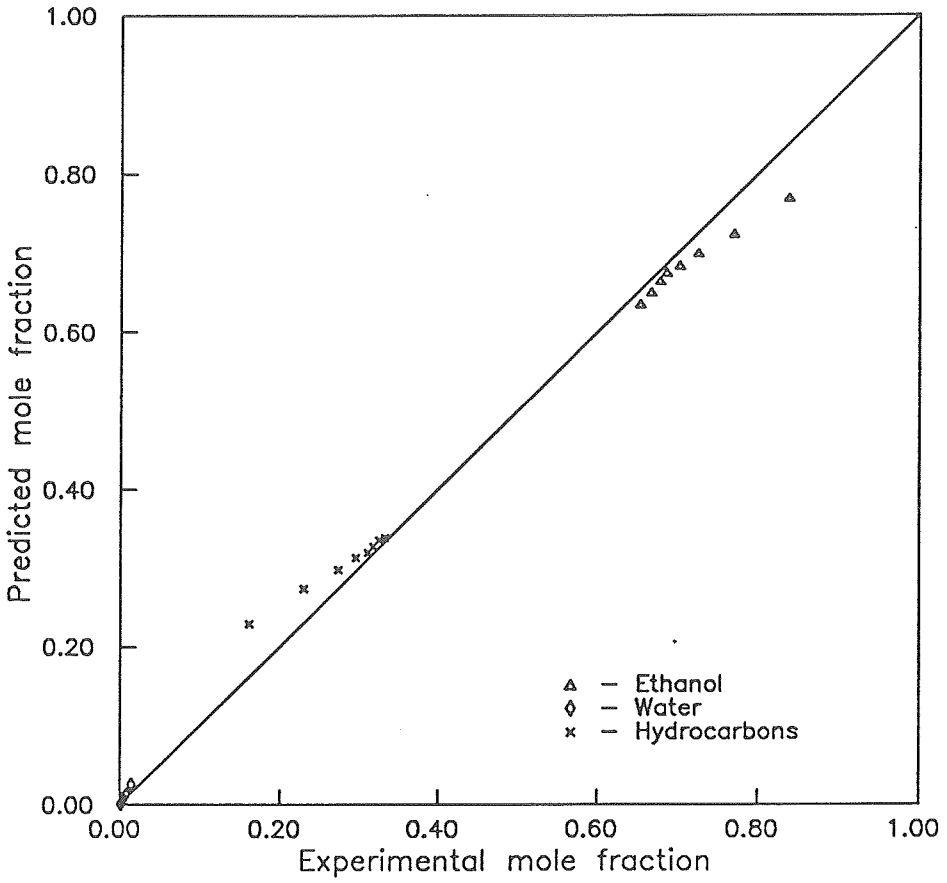

Figure 4.8: Comparison of predicted and experimental compositions (Run 8, Cairns and Furzer, 1987a).

More details of comparison for one set of data are given in Tables 4.7 and 4.8. The standard deviations of these three heterogeneous liquid models are also listed in Tables 4.9 and 4.10. The agreement of predicted compositions with experimental data is quite good, especially for Model IV, the dispersed liquid model. This is expected because the dispersed liquid model more closely models the performance on the tray. It is, of course, also the most complicated model so that it is more difficult to get the convergent solutions comparing to the other three models we used in this investigation. Comparing the results obtained from Model II and Model III, the latter is a little better than the former. Figures 4.15 and 4.16 showed the predicted total compositions obtained from Model I for Run 1 and Run 2 respectively. Model I, which treats two liquid phases as a single homogeneous liquid, is the worst when compared with the other heterogeneous liquid models. This conclusion is not surprising to us because the assumptions in this model are too far from the real situation on the tray.

4.5.2 Discussion

Mass Transfer Coefficient

As we mentioned before, the calculation of mass transfer coefficients is a key step of the simulation with a nonequilibrium model. We can use either empirical correlations (see Chapter 2) or theoretical models to calculate the mass transfer coefficients and fluxes. In this study it is the first try to apply the theoretical models, the jet-bubble and the drop model, to find out the mass transfer coefficients and fluxes. From the equations (4.28), (4.29) and (4.35), the binary pair mass transfer coefficients are dependent on physical properties of components, such as, diffusivity, and hydrodynamic characteristics, for example, dispersed gas/drop size, velocity and residence time. The values of jet/bubble diameter, population percentage and fall/rise velocity chosen are mentioned in Section 4.2.1.

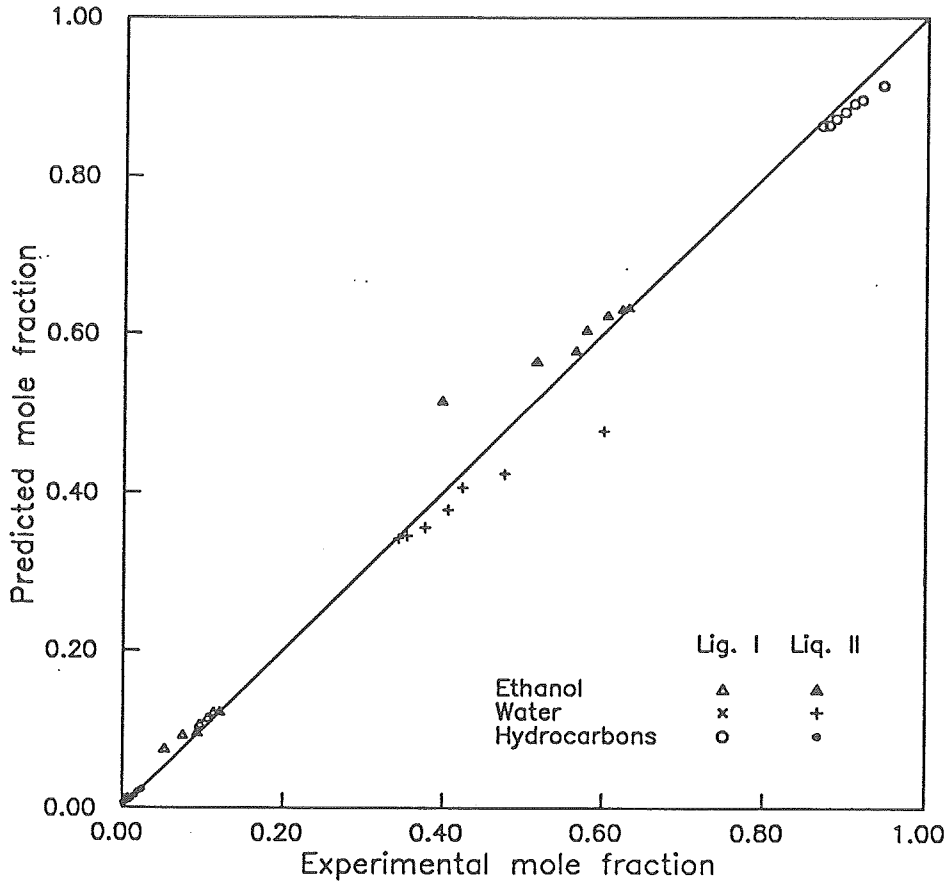

Figure 4.9: Comparison of predicted and experimental compositions for model II (Run 1, Cairns and Furzer, 1987a).

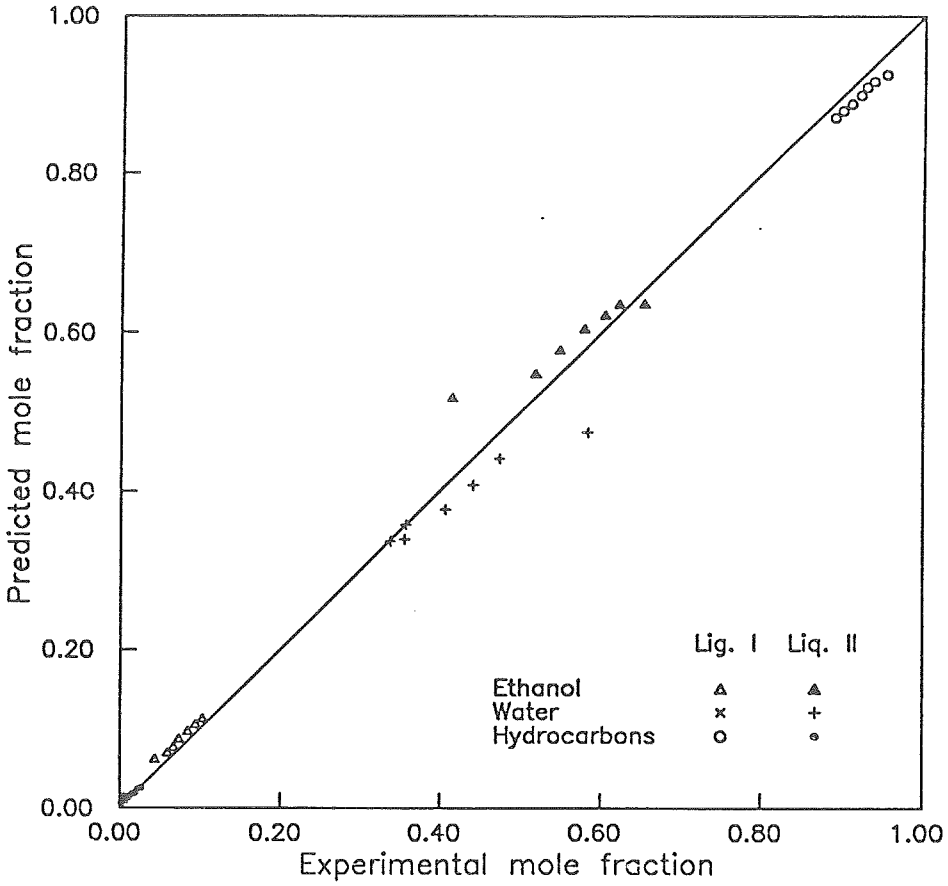

Figure 4.10: Comparison of predicted and experimental compositions for model II (Run 2, Cairns and Furzer, 1987a).

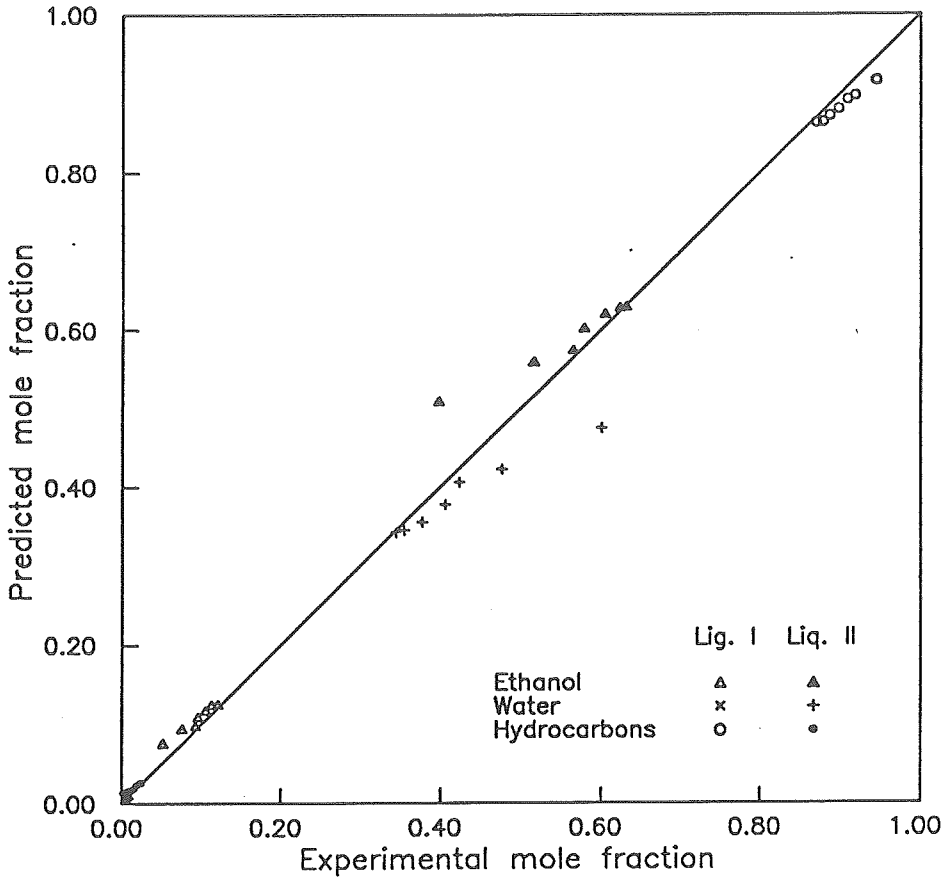

Figure 4.11: Comparison of predicted and experimental compositions for model III (Run 1, Cairns and Furzer, 1987a).

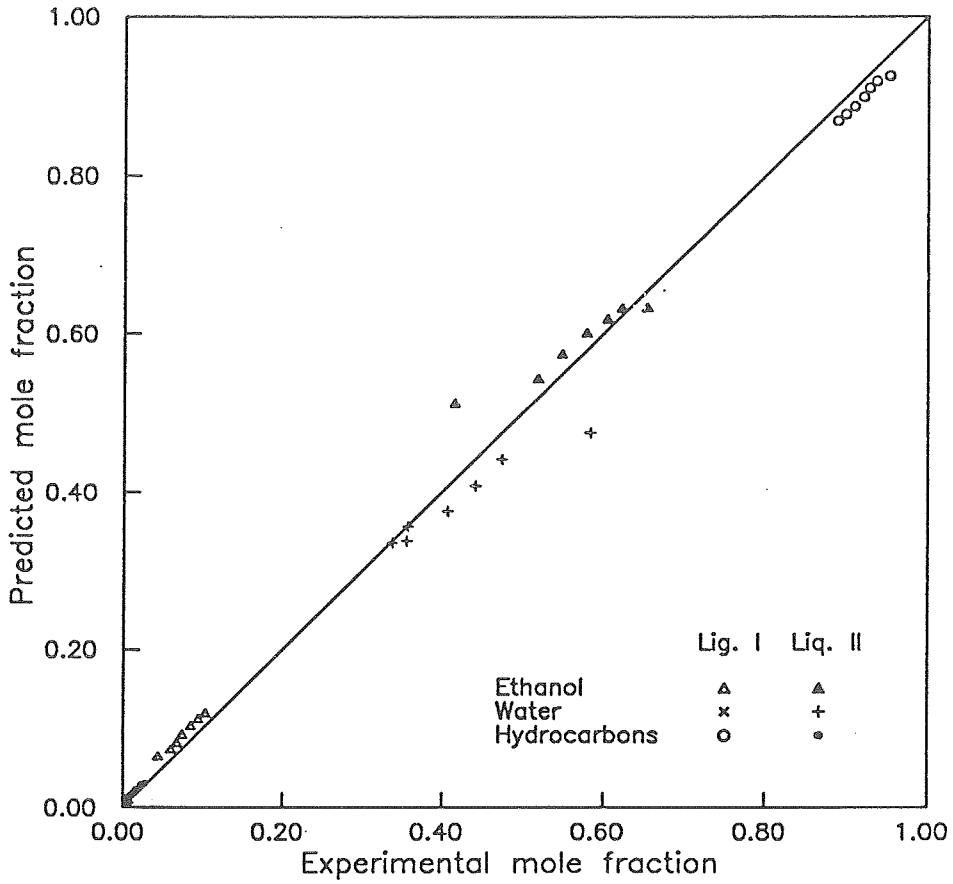

Figure 4.12: Comparison of predicted and experimental compositions for model III (Run 2, Cairns and Furzer, 1987a).

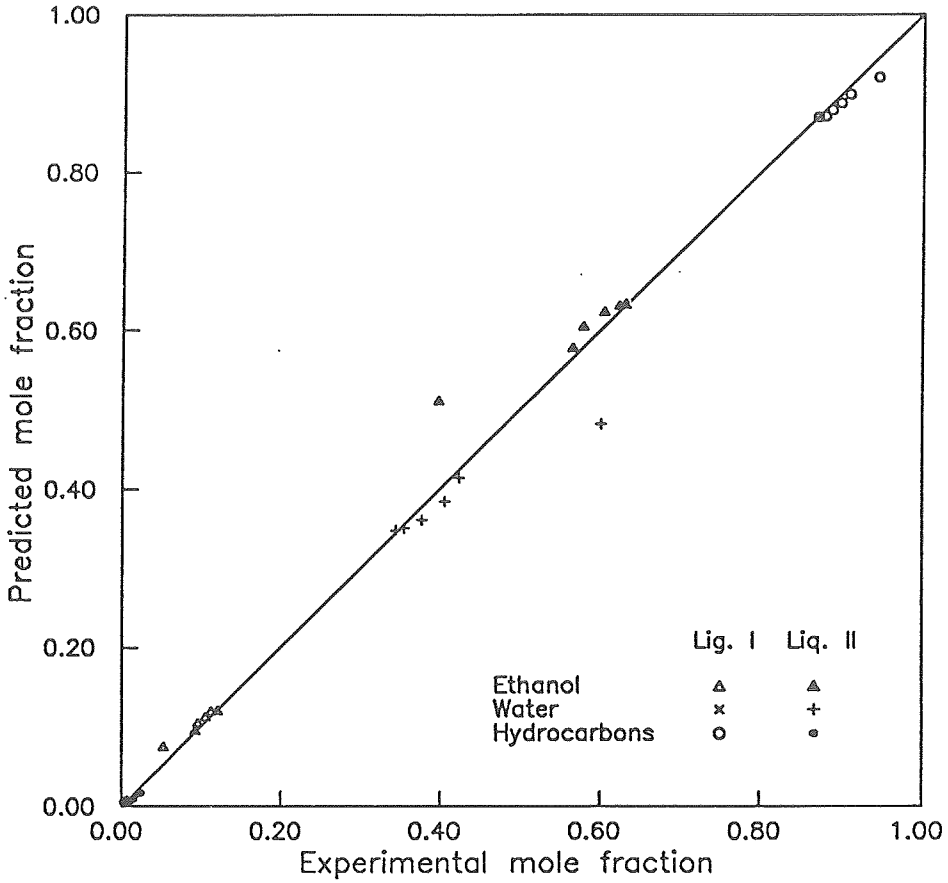

Figure 4.13: Comparison of predicted and experimental compositions for model IV (Run 1, Cairns and Furzer, 1987a).

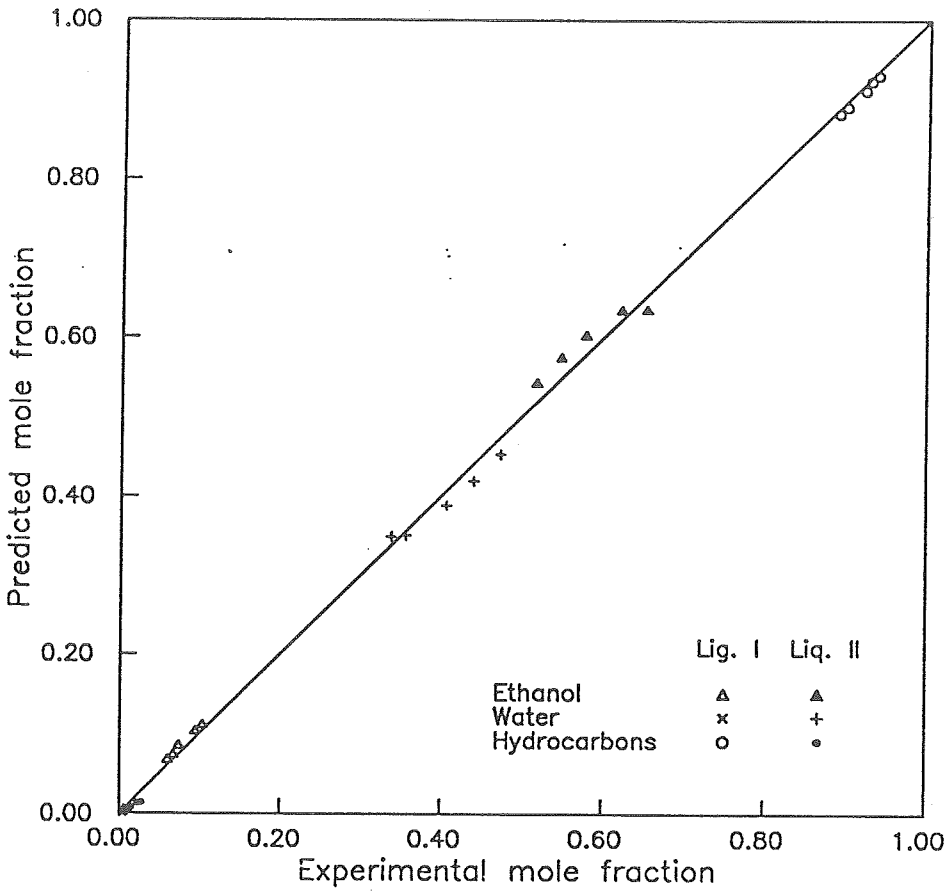

Figure 4.14: Comparison of predicted and experimental compositions for model IV (Run 2, Cairns and Furzer, 1987a).

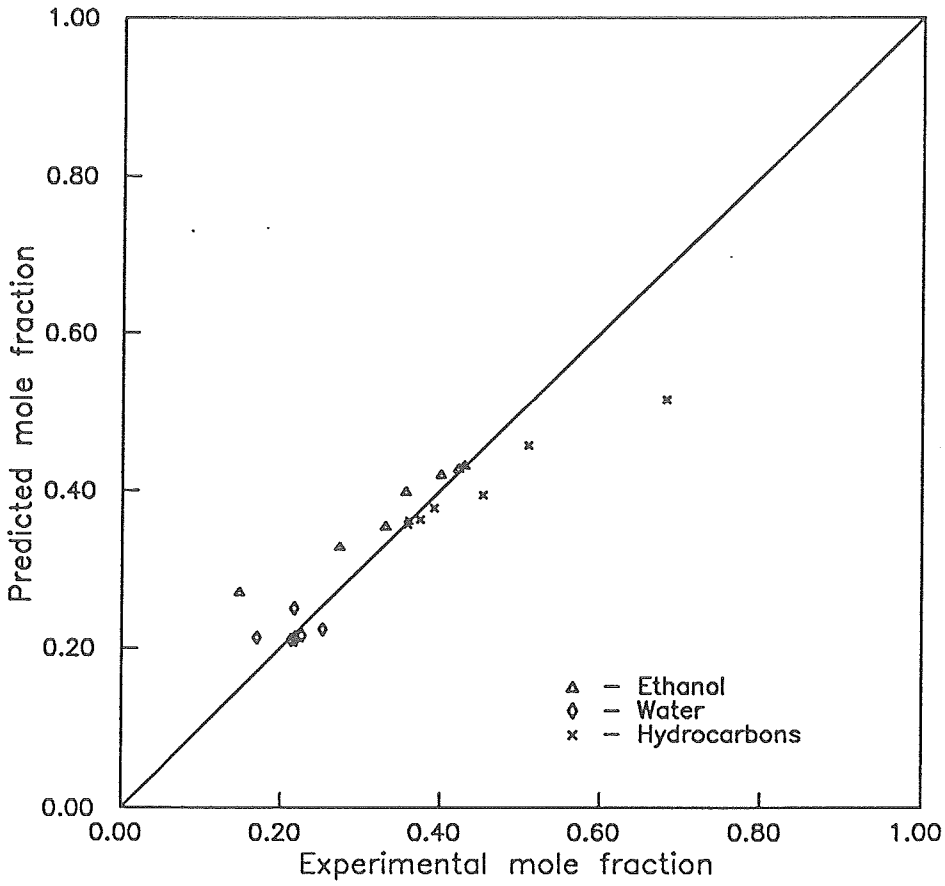

Figure 4.15: Comparison of predicted and measured total compositions for model I (Run 1, Cairns and Furzer, 1987a).

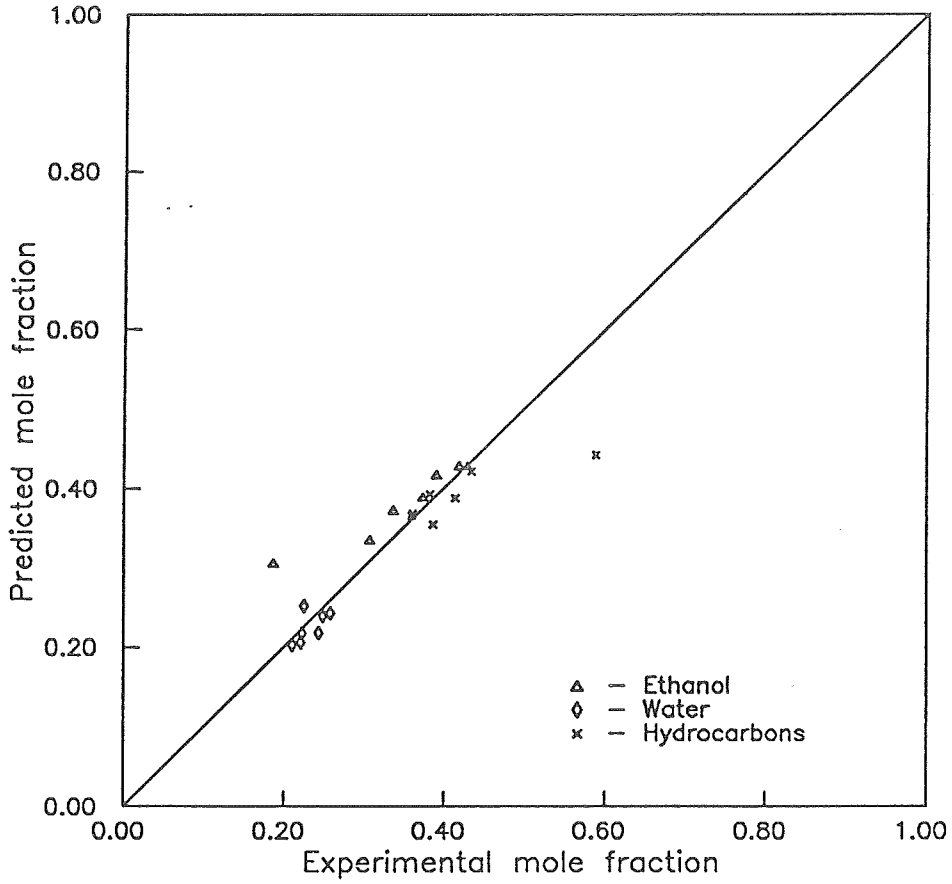

Figure 4.16: Comparison of predicted and measured total compositions for model I (Run 2, Cairns and Furzer, 1987a).

Residence time is an important factor affecting the mass transfer coefficients and average driving force shown in the equations (4.28), (4.29), (4.35) and (4.66-4.68). The experiments are carried out on trays without downcomer, and there are few correlations for estimating the froth height for this kind of the tray. We used the correlations published by Mahendru (1979) to predict the froth height with the results that the predicted froth height was a factor of 2 greater than the measured froth height mentioned in Cairns paper. It seems different material systems could cause significantly different performance. Mahendru used air as the dispersed gas, which can be considered noncondensable gas at room temperature; operation in this condition leads to increased froth height. So we decreased the froth height predicted with Mahendru's correlations by 50% when residence time is calculated.

For the drop model, the fall/rise velocity of drops is estimated by

$$u_{drop} = \frac{s}{t_{drop}} \tag{4.70}$$

where s is the average length of drop passing, the value taken ten times of drop diameter, t is the residence time of liquid phase on the tray.

From Figures 4.7-4.8 and Tables 4.4-4.5, we can conclude that the parameters used in this model are reasonable and the homogeneous liquid model is reliable for two phase distillation simulation.

The matrix $[\beta]$ in Equation (4.64) is a bootstrap matrix which portrays the non-equimolar characters of the systems considered. The molar latent heats of vaporization are different for the components tested in this simulation, however, this matrix still can be negligible without significant change for simulation results. In our simulation we consider a non-equimolar transfer but ignore the bootstrap matrix, only for reasonable simplification.

We also found that much better agreement between experimental and simulation results could be obtained by using a fixed factor for systematically modifying the interfacial area. The value of the fixed factor is better taken as 0.1 rather than 0.3, or other values.

Thermodynamic Interaction Parameters

In our simulations, the UNIQUAC model is used to calculate the activity coefficients in the liquid phase. We found that the numerical computations are *very* sensitive to the interaction parameters due to the very high nonlinearity of the thermodynamic properties such as K-values and enthalpies. The routines applied in our simulation allow us separately to use different set of interaction parameters for vapor-liquid (VL) and liquid-liquid (LL) equilibrium data, even for different pair of vapor-liquid phase calculation. That means our programs have more flexibility to handle the VL and LL equilibrium calculation. There are three sets of interaction parameters separately used to fit two independent vapor-liquid equilibrium data and one liquid-liquid equilibrium data. These parameters come from the Vapor-liquid Equilibrium Data Collection (Gmehling, Onken and Arlt, 1981, 1/1a, p157; 1/2c, p468), Liquid-liquid Equilibrium Data Collection (Sørensen, and Arlt, 1980, V/2, p386-387). We also used UNIFAC method to find out some pairs of UNIQUAC parameters since the parameters are lacking for the system tested by Cairns and Furzer.

Table 4.6: Specifications and Results of Stage 4 (Run 8, Cairns and Furzer, 1987a).

Component	Feed Flow Rate $(kmol/s)$
Ethanol	$0.1269 \times (10)^{-3}$
Water	$0.1446 \times (10)^{-5}$
Hydrocarbons	$0.6177 \times (10)^{-4}$

Component	Compositions $(mole\ fraction)$	
	Experiment	Simulation
Ethanol	0.6782	0.6651
Water	0.0044	0.0074
Hydrocarbons	0.3174	0.3275

Table 4.7: Specifications and Results of Stage 2 (Run 1, Cairns and Furzer, 1987a).

Component	Feed Flow Rate $(kmol/s)$		
	Vapor	Liquid I	Liquid II
Ethanol	$0.7212 \times (10)^{-4}$	$0.7797 \times (10)^{-5}$	$0.6432 \times (10)^{-4}$
Water	$0.3538 \times (10)^{-4}$	$0.6692 \times (10)^{-6}$	$0.3471 \times (10)^{-4}$
Hydrocarbons	$0.5891 \times (10)^{-4}$	$0.5632 \times (10)^{-4}$	$0.2594 \times (10)^{-5}$

Component	Compositions of Vapor (*mole fraction*)			
	Exp.	Model II	Model III	Model IV
Ethanol	0.4289	0.4345	0.4345	0.4341
Water	0.2123	0.2148	0.2132	0.2163
Hydrocarbons	0.3588	0.3507	0.3523	0.3496

Component	Compositions of Liquid I (*mole fraction*)			
	Exp.	Model II	Model III	Model IV
Ethanol	0.1197	0.1223	0.1259	0.1209
Water	0.0103	0.0140	0.0107	0.0091
Hydrocarbons	0.8700	0.8637	0.8634	0.8700

Component	Compositions of Liquid II (*mole fraction*)			
	Exp.	Model II	Model III	Model IV
Ethanol	0.6312	0.6333	0.6309	0.6341
Water	0.3444	0.3426	0.3421	0.3486
Hydrocarbons	0.0244	0.0241	0.0270	0.0173

Table 4.8: Specifications and Results of Stage 2 (Run 2, Cairns and Furzer, 1987a).

Component	Feed Flow Rate $(kmol/s)$		
	Vapor	Liquid I	Liquid II
Ethanol	$0.1348 \times (10)^{-3}$	$0.1359 \times (10)^{-4}$	$0.1212 \times (10)^{-3}$
Water	$0.6512 \times (10)^{-4}$	$0.1231 \times (10)^{-5}$	$0.6389 \times (10)^{-4}$
Hydrocarbons	$0.1139 \times (10)^{-3}$	$0.1085 \times (10)^{-3}$	$0.5391 \times (10)^{-5}$

Component	Compositions of Vapor $(mole\ fraction)$			
	Exp.	Model II	Model III	Model IV
Ethanol	0.4290	0.4321	0.4336	0.4298
Water	0.2102	0.2116	0.2078	0.2148
Hydrocarbons	0.3608	0.3563	0.3584	0.3554

Component	Compositions of Liquid I $(mole\ fraction)$			
	Exp.	Model II	Model III	Model IV
Ethanol	0.1024	0.1140	0.1220	0.1119
Water	0.0088	0.0165	0.0101	0.0082
Hydrocarbons	0.8888	0.8694	0.8679	0.8799

Component	Compositions of Liquid II $(mole\ fraction)$			
	Exp.	Model II	Model III	Model IV
Ethanol	0.6357	0.6370	0.6330	0.6368
Water	0.3376	0.3372	0.3360	0.3493
Hydrocarbons	0.0267	0.0258	0.0310	0.0138

Table 4.9: Standard Deviation of Three Heterogeneous Models for Run 1 (Cairns, 1987).

Component	Vapor Phase (*mol.%*)		
	Model II	Model III	Model IV
Ethanol	5.77	5.58	5.56
Water	2.77	2.52	2.78
Hydrocarbons	7.90	7.31	7.67
Component	Liquid I (*mol.%*)		
	Model II	Model III	Model IV
Ethanol	1.32	1.55	1.18
Water	0.51	0.18	0.08
Hydrocarbons	1.88	1.79	1.27
Component	Liquid II (*mol.%*)		
	Model II	Model III	Model IV
Ethanol	5.02	4.74	4.89
Water	5.32	5.37	4.98
Hydrocarbons	0.32	0.72	0.56

Table 4.10: Standard Deviation of Three Heterogeneous Models for Run 2 (Cairns, 1987).

Component	Vapor Phase (*mol.%*)		
	Model II	Model III	Model IV
Ethanol	5.23	5.16	2.19
Water	1.59	1.60	0.73
Hydrocarbons	6.44	6.22	2.01

Component	Liquid I (*mol.%*)		
	Model II	Model III	Model IV
Ethanol	1.38	1.85	1.01
Water	0.69	0.21	0.28
Hydrocarbons	2.11	2.11	0.74

Component	Liquid II (*mol.%*)		
	Model II	Model III	Model IV
Ethanol	4.49	4.15	2.24
Water	4.63	4.62	1.62
Hydrocarbons	0.25	0.70	0.87

4.6 Summary

Four nonequilibrium stage models, the homogeneous liquid model, the segregated liquid model, the stratified liquid model and the dispersed liquid model, have been developed for the simulation of three phase distillation. The features of these models are outlined as follows:

1. The mass conservation equations are split into two parts, one for each phase. The mass and energy balances around the interfaces are connected with these equations and assumed that the interface be continuous and at thermodynamic equilibrium.

2. The process of mass transfer through the interface is modelled based on a theoretical model, jet-bubble or drop model.

3. As soon as the material stability judgement has been done, one of the four models mentioned in Section 4.3 can be arbitrarily chosen. In each of these models only two phase contacting is involved, there are none of the difficulties associated with three phase equilibrium calculations. That does not mean that the nonequilibrium calculations are simple to converge; just that the numerical difficulties differ from those encountered with equilibrium models.

4. The equations modelling a three phase tray were solved using various tearing strategies. The VL and LL equilibrium equations (bubble point, dew point and phase split calculations) are done by solving the relevant subset of equations using a multidimensional Newton's method.

5. The models allow us to choose different models and different set of the interaction parameters to calculate activity coefficients and K-values. The calculations are very sensitive to the composition and temperature for very highly nonideal liquid mixture which is met in three phase distillation.

As far as we are aware, this is the first time the rate-based models of three phase distillation have been described. Reasonably good agreement between experimental data and simulation prediction was obtained, especially from the dispersed liquid model.

Chapter 5

Conclusion

5.1 Conclusion

In this project nonequilibrium models have been proposed for simulating multiphase multicomponent separation processes.

Specifically:

1. The nonequilibrium stage model developed by Krishnamurthy and Taylor (1985a) has been used to simulate vapor-liquid distillation in two packed columns (Arwikar, 1981 and Gorak, 1985) and one sieve tray column (Hauer, 1948). The agreement between predicted results and measured data is very good.

2. This nonequilibrium stage model has been adopted to simulate liquid-liquid extraction processes. Four sieve tray extraction columns (Pyle, 1950; Garner, 1953 and Rocha, 1984) have been simulated with this model, again with good results.

3. Four rate-based models, one for homogeneous liquid and three for heterogeneous liquid, have been developed for vapor-liquid-liquid distillation. This is the first time three phase distillation processes have been simulated with nonequilibrium models. The results obtained from the simulation of Cairns and Furzer (1987a) experimental data evidence that these models are encouraging.

It may be worth emphasizing once more that the nonequilibrium model has been successfully used to simulate multiphase multicomponent separation processes, for example, two and three phase distillation and liquid-liquid extraction in packed columns and tray columns.

In the calculation of mass transfer coefficients, an important part of the nonequilibrium model, the jet-bubble model and the drop model, which were applied to three phase distillation, led to very good agreement between the measured and predicted

compositions. These models are useful for estimating mass transfer coefficients when the empirical correlations are lacking. There is considerable scope for improving the model predictions by tuning parameters, such as the jet/bubble/drop size and its population distribution, something we have not attempted to do.

5.2 Suggestions for Further Work

Firstly, simulation of just a single three phase tray has been carried out with the models mentioned in Chapter 4. Much further testing is required but we believe that the models proposed here can serve as a framework for developing better models capable of true predictions of three phase distillation. The next step would be to develop a procedure for simulating an entire three phase distillation column.

The greater need, however, is not for more simulation studies but for more experimental data that can be used to test any model of three phase distillation.

Nomenclature

A	active bubbling area of a tray, m^2
a	interfacial area per unit volume of froth, $\frac{m^2}{m^3}$
a'	interfacial area per unit volume of dispersed gas, $\frac{m^2}{m^3}$
a_e	effective packing surface, $\frac{m^2}{m^3}$
a_p	packing surface, $\frac{m^2}{m^3}$
a_t	total surface area of packing, m^2
a_w	wetted surface area of packing, m^2
B	backmixing ratio of flow rate for liquid-liquid extraction
c	the number of components
c_t	mixture molar density, $\frac{kmol}{m^3}$
D	diffusion coefficient, $\frac{m^2}{s}$
$Đ_{ij}$	Maxwell-Stefan diffusivity of pair i-j in multicomponent mixture, $\frac{m^2}{s}$
$Đ_{ref}$	reference value of Maxwell-Stefan diffusivity, $\frac{m^2}{s}$
d	diameter, m
d_{eq}	equivalent diameter of channel dependent on geometric size of packing, m
d_h	diameter of holes, m
E	energy transfer flux, $\frac{kcal}{m^2 s}$
F	molar flow rate of the feed, $\frac{kmol}{s}$
f_k	fraction of vapor entering bulk froth zone which is transported by the k-th bubble size population
Fo	Fourier number
Fr	Froude number
G	total Gibbs free energy, $kcal$
G	molar Gibbs free energy, $\frac{kcal}{kmol}$
G_V	superficial mass velocity of vapor, $\frac{kg}{m^2 s}$

G_L	superficial mass velocity of liquid, $\frac{kg}{m^2 s}$
g	acceleration due to gravity, $\frac{m}{s^2}$
g_c	conversion factor (=1.0 in SI units)
H	enthalpy, $\frac{kcal}{kmol^0 K}$
H_t	plate spacing, m
h	distance parameter measured from tray floor, m
h_c	height of coalescence zone, m
h_f	height of bulk froth zone, m
h_I	height of formation zone, m
h_{II}	height of bulk rise zone, m
$[J]$	Jacobian matrix
J_o	zero order Bessel function
j_m	root of $J_o(j_m) = 0$
K	distribution coefficient
k	mass transfer coefficient, $\frac{m}{s}$
$[K^{eq}]$	diagonal matrix of equilibrium K-values
$[k^*]$	the matrix of mass transfer coefficients, $\frac{m}{s}$
L	molar flow rate of the liquid phase, $\frac{kmol}{s}$
N	molar flux, $\frac{kmol}{m^2 s}$
n	the number of stages (or sections)
p	pressure, atm
p^0	saturated vapor pressure, atm
Q	heat exchange with the environment, $\frac{kcal}{s}$
q	conductive heat flux, $\frac{kcal}{m^2 s}$
$[Q]$	matrix defined by equations(4.67) to (4.69)
$[R]$	matrix of inverted mass transfer coefficient, $\frac{s}{m}$
Re	Reynolds number

s	ratio of sidestream to the interstage flow rate
Sc	Schmidt number
Sh	Sherwood number
T	temperature, ^0K
t	residence time, s
U_c	superficial velocity of continuous liquid phase, $\frac{m}{s}$
U_d	superficial velocity of dispersed liquid phase, $\frac{m}{s}$
U_o	velocity through orifices, $\frac{m}{s}$
U_s	liquid-liquid slip velocity, $\frac{m}{s}$
U_{dow}	liquid velocity in downcomer, $\frac{m}{s}$
u	velocity, $\frac{m}{s}$
u_s	superficial velocity, $\frac{m}{s}$
V	molar flow rate of the vapor phase, $\frac{kmol}{s}$
We	Weber number
x	mole fraction in liquid phase
y	mole fraction in vapor phase
z_i	mole fraction in the feed

Greek letters

α	liquid phase ratio to feed
$[\beta]$	bootstrap matrix with elements given by equation (4.64)
$[\Gamma]$	matrix of thermodynamic factors defined by equation (2.15)
γ	activity coefficient
δ_{ij}	Kronecher delta
η	Murphree efficiency
α	phase-splitting parameter
λ	molar latent heat of vaporization, $\frac{kcal}{kmol}$
μ	viscosity, $\frac{kg}{ms}$
$[\Xi]$	the matrix of correction factor
ξ	the dimensionless film length
ρ	density, $\frac{kg}{m^3}$
$[\varrho]$	the matrix of second derivatives of Gibbs free energy
σ	surface tension, $\frac{kg}{s^2}$
ϕ	operational holdup
$[\Phi]$	the matrix of dimensionless mass transfer rate factors

Subscript:

av	average value
c	number of component
E	enter vapor mixture
eff	effective value
I	interface
i, j, l	component
j	stage numbering
L	vapor mixture leaving tray
L,V	liquid and vapor phases
I and II	referring to zone I and zone II respectively
II_k	referring to the k-th bubble population in zone II

Superscript

$'$ and $''$	different liquid phases
$-$	average
$*$	equilibrium value
c	continuous phase
d	dispersed phase
L	liquid phase
o	infinite dilution parameter
OV	overall vapor phase parameter
V	vapor phase

References

1. Ashley, M.J., and G.G. Haselden, "Effectiveness of Vapor-Liquid Contacting on a Sieve Plate", *Trans. Inst. Chem. Engrs.*, 50, 119, 1972.

2. Ashton, N.A., A. Arrowsmith, C.J. Yu, "Distillation Hydraulics with Immiscible Liquids", IchemE Symposium Series, Distillation and Absorption, No.104, B113, 1987.

3. Arwickar, K.J., Ph. D. Dissertation, University of California Santa Barbara, 1981.

4. Baden, N., and M. Michelsen, "Computer Methods for Steady-State Simulation of Distillation Columns", IChemE Symposium Series, Distillation and Absorption, No. 104, A425, 1987.

5. Bennett, D.L., R. Agrawal, and P.J. Cook, " New Pressure Drop Correlation for Sieve Tray Distillation Columns", *AIChE J.*, 29(3), 434, 1983.

6. Block, U., and B. Hegner, "Development and Application of a Simulation Model for Three-Phase Distillation", *AIChE J.*, 22(3), 582, 1976.

7. Bloomfield, A.L., Discussion in Underwood's paper, "The Determination of Plate Efficiency in Fractionating Mixtures", *Trans Inst. Chem. Engrs.* (London), 12 140, 1934.

8. Boston, J.F., and V.B. Shah, "An Algorithm for Rigorous Distillation Calculations with Two Liquid Phases", presented at 86th National meeting of AIChE, Houston, April, 1979.

9. Bravo, J.L., Rocha, J.A., and Fair, J.R., "Mass Transfer in Gauze Packings", *Hydrocarbon Processing*, January, 91, 1985.

10. Burgess, J.M., and Calderbank, P.H., "The Measurement of Bubble Parameters in Two-Dispersions-II The Structure of Sieve Tray Froths", *Chem. Eng. Sci.*, 30, 1107, 1975.

11. Cairns, B.P., and I.A. Furzer, "Three - Phase Azeotropic Distillation. Experimental Results", IChemE Symposium Series, Distillation and Absorption, No.104, B505, 1987a.

12. Cairns, B.P., and I.A. Furzer, "Azeotropic Distillation - Simulation and Experiment", Chemeca, 87, 57.1, 1987b.

13. Cairns, B.P., and I.A. Furzer, "Sensitivity Testing with the Predictive Thermodynamic Models NRTL, UNIQUAC, ASOG, and UNIFAC in Multicomponent Separations of Methanol-Acetone-Chloroform", *Chem. Eng. Sci.*, 43(3), 495, 1988.

14. Cairns, B.P., A Ph. D. dissertation, The University of Sydney, July, 1988.

15. Cha, Tai-Hsing and Prausnitz, J. M., "Thermodynamic Method for Simultaneous Representation of Ternary Vapor-Liquid and Liquid-Liquid Equilibria", *Ind. Eng. Chem. Proc. Des. Dev.*, 24, 551, 1985.

16. Chan, H., and J.R. Fair, "Prediction of Point Efficiencies on Sieve Trays. 1. Binary Systems", *Ind. Eng. Chem. Pro. Des. Dev.*, 23, 814, 1984a.

17. Chan, H., and J.R. Fair, "Prediction of Point Efficiencies on Sieve Trays. 2. Multicomponent Systems", *Ind. Eng. Chem. Pro. Des. Dev.*, 23, 814, 1984b.

18. Clark, F.W., Discussion in Guinot's paper, "Azeotropic Distillation in Industry", *Trans. Inst. Chem. Engrs.*, 16, 197, 1938.

19. Colburn, A.P., and J.C. Phillips, "Experimental Study of Azeotropic Distillation - Use of Trichloroethylene in Dehydration of Ethanol", *Trans Am. Inst. Chem. Engrs.*, 40, 333, 1944.

20. Davies, B., Z. Ali, K.E. Porter, "Distillation of Systems Containing Two Liquid Phases", *AIChE J.*, 33, 161, 1987.

21. Deam, J.R., and Maddox, R.N., "How to Figure Three-Phase Flash", *Hydrocarbon Processing*, July 163, 1969.

22. Dongen, D.B.V., M.F. Doherty, and J.R. Haight, "Material Stability of Multicomponent Mixtures and the Multiplicity of Solutions to Phase-Equilibrium Equations. Nonreacting Mixtures", *Ind. Eng. Chem. Fundam.*, 22, 472, 1983.

23. Eldridge, R.B., J.L. Humphrey, and J.R. Fair, *Proc. Int. Solvent Extraction Conf.*, Munich, 3, 55 (1986)

24. Fair, J.R., "Tray Hydraulics Perforated Trays", Chapter 15, **Design of Equilibrium Stage Progresses**, Smith, B.D. (editor), McGraw-Hill, New York, 1963.

25. Fair, J.R., "Distillation: whither, not whether", IChemE Symposium Series, Distillation and Absorption, No.104, A613, 1987.

26. Ferraris G.B., and M. Morbidelli, "Distillation Models for Two Partially Immiscible Liquids", *AIChE J.*, 27, 881, 1981.

27. Ferraris G.B., and M. Morbidelli, "An Approximate Mathematical Model for Three-Phase Multistage Separators", *AIChE J.*, 28(1), 49, 1982.

28. Fuchs, R., M. Gipser, and J. Gaube, "Calculation of Ternary Vapor-Liquid-Liquid Equilibria for Design of Three-Phase Distillation", *Fluid Phase Equilibria*, 14, 325, 1983.

29. Furzer, I., "Ethanol Dehydration Column Efficiencies Using UNIFAC", *AIChE J.*, 31(8), 1389, 1985.

30. Garner, F. H., S.R.M. Ellis, and D.W. Fosbury, "Perforated Plates in Liquid-liquid Extraction: Toluene - Diethylamine - Water System", *Trans. Inst. Chem. Engrs.*, 31, 348, 1953.

31. Gerster, J.A., T. Mizushina, T.N. Marks, and A.W. Catanach, "Plant Performance of a 13-ft.-diameter Extractive-Distillation Column",*AIChE J.*, 1, 536, 1955.

32. Gmehling, J., U. Onken, and W. Arlt, **Vapor-Liquid Equilibrium Data Collection**, DECHEMA, 1982.

33. Goodliffe, A.H., "The Practical Testing of a Continuous Petroleum Still", *Trans Inst. Chem. Engrs.*, 12, 107, 1934.

34. Gorak, A., and Vogelpohl, A., "Experimental Study of Ternary Distillation in a Packed Column", *Separation Science and Technology*, 20(1), 33, 1985.

35. Goto, S., and M. Matsubara, "Combined Process of Reaction, Extraction and Distillation in a Multistage Column", *J. Chem. Eng. Japan*, 11(5), 384, 1978.

36. Grohse, E.W., R.F. McCartney, H.J. Hauer, J.A. Gerster, and A.P. Colburn, *Chem. Eng. Prog.*, 45, 725, 1949.

37. Grohse, E.W., "Plate Efficiencies in the Separation of C_4 Hydrocarbons by Extractive Distillation", Ph.D. Dissertation, University of Delaware, 1948.

38. Guinot, H., and F.W. Clark, "Azeotropic Distillation in Industry", *Trans Inst. Chem. Engrs.*, 16, 189, 1938.

39. Happel, J., et al., "Extractive Distillation-Separation of C_4 Hydrocarbons Using Furfural", *Trans Am. Inst. Chem. Engrs.*, 42, 189, 1946.

40. Hauer, H.J., "The Effect of Average Column Temperature upon the Plate Efficiency in the Separation of Isobutane and 1-Butene by Extractive Distillation with Dry Furfural", A Master thesis, The University of Delaware, 1948.

41. Henley, E.J., and J.D. Seader, **Equilibrium Stage Separation Operations in Chemical Engineering**, Wiley, New York, 1981.

42. Herron, C.C.Jr., B.K. Kruelskie, J.R. Fair, "Hydrodynamics and Mass Transfer on Three-phase Distillation Trays", *AIChE J.*, 34, 1267, 1988.

43. Hofer, H., "Influence of Gas-phase Dispersion on Plate Column Efficiency", *Ger. Chem. Eng.*, 6, 113, 1983.

44. Holland, C.D., **Fundamentals of Multicomponent Distillation**, McGraw-Hill, New York 1981.

45. Holland, C.D., **Fundamentals and Modeling of Separation Processes**, Prentice-Hall, Englewood Cliffs, NJ 1975.

46. Kaltenbacher, E., "On the Effect of the Bubbles Size Distribution and the Gas-Phase Diffusion on the Selectivity of Sieve Trays", *Chem. Eng. Fund.*, 1(1), 47, 1982.

47. Kastanek, F., and G. Standart, **Efficiency of Distillation Trays**, Academia, Czechoslovak Academy of Sciences Press, Prague, 1966.

48. Keyes, D.B., "The Manufacture of Anhydrous Ethyl Alcohol", *Ind. Eng. Chem.*, 21, 998, 1929.

49. King, C.J., **Separation Processes**, McGraw-Hill, New York, 1980.

50. Kingsley, J.P., and A. Lucia, "Simulation and Optimization of Three-phase Distillation Processes", *Ind. Eng. Chem. Res.*, 27, 1900, 1988.

51. Kinoshita, M., I. Hashimoto, and T. Takamatsu, "A New Simulation Procedure for Multicomponent Distillation Column Processing Nonideal Solutions or Reactive Solutions", *J. Chem. Eng. Jap.*, 16(5), 370, 1983.

52. Konstantinov, E.N., Dissertation, MIKhM, 1960, cited by Gorak, 1985.

53. Kovach III, J.W., and W.D. Seider, "Heterogeneous Azeotropic Distillation: Experimental and Simulation Results", *AIChE J.*, 33(8), 1300, 1987.

54. Kovach III, J.W., and W.D. Seider, "Heterogeneous Azeotropic Distillation - Homotopy - Continuation Methods", *Comput. Chem. Eng.*, 11(6), 593, 1987.

55. Krishna, R., "A Generalized Film Model for Mass Transfer in Nonideal Fluid Mixtures", *Chem. Eng. Sci.*, 32, 659, 1977.

56. Krishna, R., "Model for Prediction of Point Efficiencies for Multicomponent Distillation", *Chem. Eng. Des.*, 63, September, 1985.

57. Krishna, R., C.Y. Lo, C. Olivera-Fuentes, D.M.T. Newsham, and G.L. Standart, "Ternary Mass Transfer in Liquid-Liquid Extraction", *Chem. Eng. Sci.*, 40, 893, 1985.

58. Krishna, R., S.M. Nanoti, and A.N. Goswami, "Mass-Transfer Efficiency of Sieve Tray Extraction Columns", *Ind. Eng. Chem. Res.*, 28, 642, 1989.

59. Krishna, R., and R. Taylor, Chapter 7 in Handbook of **Heat and Mass Transfer Operations**, Volume 2, Gulf Publishing Company, Houston, 1986.

60. Krishnamurthy, R., and R. Taylor, "A Nonequilibrium Stage Model of Multicomponent Separation Processes Part 1: Model Description and Method of Solution", *AIChE J.*, 31(3), 449, 1985a.

61. Krishnamurthy, R., and R. Taylor, "A Nonequilibrium Stage Model of Multicomponent Separation Processes Part II: Comparison with Experiment", *AIChE J.*, 31(3), 456, 1985b.

62. Krishnamurthy, R., and R. Taylor, "A Nonequililbrium Stage Model of Multicomponent Separation Processes Part III: The Influence of Unequal Component Efficiencies in Process Design Problems", *AIChE J.*, 31(12), 1973, 1985c.

63. Krishnamurthy, R., and R. Taylor, "Simulation of Packed Distillation and Absorption Columns", *Ind. Eng. Chem. Process Des. Dev.* 24, 513, 1985d.

64. Krishnamurthy, R., and R. Taylor, "Absorber Simulation and Design Using A Nonequilibrium Stage Model", *Can. J. Chem. Eng.*, 64, 96, 1986.

65. Kumar, A., S. Hartland, "Prediction of Drop Size Produced by a Multiorifice Distributor", *Trans. Inst. Chem. Engrs.*, 60, 35, 1982.

66. Lahiere, R. and J.R. Fair, "Mass-Transfer Efficiencies of Column Contactors in Supercritical Extraction", *Ind. Eng. Chem. Res.*, 2, 2086, 1987.

67. Lo, T.C., M.H.I. Baird, and C. Hanson, **Handbook of Solvent Extraction**, Wiley Interscience, New York, 1983.

68. Lockett, M.J., **Distillation Tray Fundamentals**, Cambridge, 1986.

69. Lockett, M.J., R.D. Kirkpatrick and M.S. Uddin, "Froth Regime Point Efficiency for Gas-Film Controlled Mass Transfer on a Two-Dimensional Sieve Tray", *Trans IChemE*, 57, 25, 1979.

70. Lockett, M.J., and M.S. Uddin, "Liquid-Phase Controlled Mass Transfer in Froths on Sieve Trays", *Trans. Inst. Chem. Engrs.*, 58, 166, 1980.

71. Lockett, M.J., and M.S. Uddin, "Effect of Non-Uniform Bubbles in the Froth the Correlation and Prediction of Point Efficiencies", *Chem. Eng. Res. Des.*, 61, March, 119, 1983.

72. Mahendru, H.L., A. Hackl, "Contribution to the Design of Sieve Trays Without Downcomers", IChemE Symposium Series, No. 56, 3.2/35, 1979.

73. Major, C.J., and R.R. Hertzog, "Flow Capacities of Sieve Plate Liquid Extraction Columns", *Chem. Eng. Prog.*, 51, 17-j, 1955.

74. Maurer, G., and J.M. Prausnitz, "Thermodynamics of Multicomponent Liquid-Liquid-Vapor Equilibria for Distillation-Column Design", IChemE Symposium Series, No. 56, 1.3/41, 1979.

75. Michelsen, M.L., Comments on "Material Stability of Multicomponent Mixtures and the Multiplicity of Solutions to Phase-Equilibrium Equations. 1. Nonreacting Mixtures", *Ind. Eng. Chem. Fundam.*, 23, 373, 1984.

76. Nagata, I., "Prediction Accuracy of Multicomponent Vapor-Liquid Equilibrium Data from Binary Parameters", *J. Chem. Eng. Jap.*, 6(1), 18, 1973.

77. Nagel, O., M. Molzahn, and G. Wickenhauser, Phase Equilibria and Fluid Properties, Part II, Dechema 169, 1980.

78. Negri, E.D. and W.J. Korchinsky, "Multicomponent Mass Transfer in Spherical Rigid Drops", *Chem. Eng. Sci.*, 41(9), 2401, 1986.

79. Niedzwiecki, J.L., R.D. Springer, and R.G. Wolfe, "Multicomponent Distillation in the Presence of Free Water", *Chem. Eng. Prog.*, 76(4), 57, 1980.

80. Ohanomah, M.O. and D.W. Thompson, "Computation of Multicomponent Phase Equilibria-Part II. Liquid-Liquid and Solid-Liquid Equilibria", *Comput. Chem. Eng.*, 8(3/4), 157, 1984.

81. Onda, K.H. Takeuchi, and Y. Okumoto, "Mass Transfer Coefficients Between Gas and Liquid Phases in Packed Columns", *J. Chem. Eng. Jap.*, 1, 56, 1968.

82. Othmer, D.F., "Acetic Acid Dehydration", *Trans Am. Inst. Chem. Engrs.*, 30, 299, 1935.

83. Poffenberger, N., L.H. Horsley, H.S. Nutting, and E.C. Britton, "Separation of Butadiene by Azeotropic Distillation with Ammonia", *Trans Am. Inst. Chem. Engrs.*, 42, 815, 1946.

84. Powers, M.F., D.J. Vickery, A. Arehole, and R. Taylor, "A Nonequilibrium Stage Model of Multicomponent Separation Processes - V. Computational Methods for Solving the Model Equations ", *Comut. Chem. Eng.*, 12(12), 1229, 1988.

85. Prado, M., J.R. Fair, "A Fundamental Model for the Prediction of Sieve Tray Efficiency", IChemE Symposium Series, Distillation and Absorption, No.104, A529, 1987.

86. Pratt, H.R.C., "Interphase Mass Transfer", Chapter 3, **Handbook of Solvent Extraction**, Lo et al., Wiley Interscience, New York, 1983.

87. Prausnitz, J., et al., **Computer Calculations for Multicomponent Vapor-Liquid and Liquid-Liquid Equilibria**, Prentice-Hall, 1980.

88. Priestly, R., and S.R.M. Ellis, "Gas agitated liquid extraction columns", *Chem. Ind.*, No. 19, 757, 1978.

89. Prokopakis, G.J., and W.D. Seider, "Feasible Specifications in Azeotropic Distillation", *AIChE J.*, 29(1), 49, 1983a.

90. Prokopakis, G.J., and W.D. Seider, "Dynamic Simulation of Azeotropic Distillation Towers", *AIChE J.*, 29(6), 1017, 1983b.

91. Prokopakis, G.J., W.D. Seider, B.A. Ross, "Azeotropic Distillation Towers with Two Liquid Phases", **Foundations of Computer Aided Chemical Process Design**, Vol.II, Mah, R.S.H., Seider W.D.(editors) AIChE, New York, 1981.

92. Pucci, A., P. Mikitenko, and L. Asselineau, "Three-Phase Distillation, Simulation and Application to the Separation of Fermentation Products", *Chem. Eng. Sci.*, 41(3), 485, 1986.

93. Pyle, C., Colburn, A.P., and Duffey, H.R., "Factors Controlling Efficiency and Capacity of Sieve-Plate Extraction Towers", *Ind. Eng. Chem.*, 42(6), 1042, 1950.

94. Reid, R.C., J.M. Prausnitz, and T.K. Sherwood, **The Properties of Gases and Liquids**, 3rd Edition, McGraw-Hill, New York, 1977.

95. Reid, R.C., J.M. Prausnitz, and B.E. Poling, **The Properties of Gases and Liquids**, 4th. Edition, McGraw-Hill, New York, 1977.

96. Rocha-Uribe, J.A., Ph.D. Dissertation, The University of Texas at Austin (1984)

97. Rocha, J.A., J.L. Humphrey, and J.R. Fair, "Mass-Transfer Efficiency of Sieve Tray Extractors", *Ind. Eng. Chem. Proc. Des. Dev.*, 25(4), 862, 1986.

98. Roche, E.C., "General Design Algorithm for Multistage Counter Current Equilibrium Processes", *Brit. Chem. Eng.*, 16, 821, 1971.

99. Ross, B., and W.D. Seider, "Simulation of Three-Phase Distillation Towers", *Comput. Chem. Eng.*, 5(1), 7, 1980.

100. Schoenborn, E.M., J.F. Koffolt, and J.H. Withrow, "Rectification in The Presence of An Insoluble Component", *Trans. Am. Inst. Chem. Engrs.*, 37, 997, 1941.

101. Schuil, J.A., and K.K. Bool, "Three-Phase Flash and Distillation", *Comput. Chem. Eng.*, 9(3), 295, 1985.

102. Seader, J.D., "Computer Modeling of Chemical Processes", *Chem. Eng. Ed.*, Spring, 88, 1985.

103. Seader, J.D., "The Rate-Based Approach for Modeling Staged Separations - A New Era", presented at ASPENWORLD 88, Amsterdam, The Netherlands, November, 1988.

104. Seibert, A.F. and J.R. Fair, "Hydrodynamics and Mass Transfer in Spray and Packed Liquid-Liquid Extraction Columns", *Ind. Eng. Chem. Res.*, 27, 470, 1988.

105. Sivasubramanian, M.S., J.F. Boston, "Rate-based Separation Process Modeling Techniques", presentation at the Annual AIChE Meeting, Washington, November, 1988.

106. Skelland, A.H.P. and W.L. Conger, "A Rate Approach to the Design of Perforated Plate Extraction Columns", *Ind. Eng. Chem. Proc. Des. Dev.*, 12, 448, 1973.

107. Skelland, A.H.P., **Diffusional Mass Transfer**, Wiley, New York, 1974.

108. Skelland, A.H.P., and Y.F. Hung, "Continuous Phase Mass Transfer During Formation of Drops From Jets", *AIChE J.*, 25, 80, 1979.

109. Smith, B.D. (editor), **Design of Equilibrium Stage Progresses**, McGraw-Hill, New York, 1963.

110. Sørensen, J.M. and W. Arlt, **Liquid-liquid Equilibrium Data Collection**, DECHEMA, 1979.

111. Swartz, C.L.E., and W.E. Stewart, "A Collocation Approach to Distillation Column Design", *AIChE J.*, 32(11), 1832, 1986.

112. Swartz, C.L.E., and W.E. Stewart, "Finite-element Steady State Simulation of Mutliphase Distillation", *AIChE J.*, 33(12), 1977, 1987.

113. Taylor, R., M.F. Powers, M. Lao, and A. Arehole, "The Development of A Nonequilibrium Model for Computer Simulation of Multicomponent Distillation and Absorption

Operations", IChemE Symposium Series, Distillation and Absorption, No.104, B321, 1987.

114. Taylor, R., R. Krishnamurthy and J.S. Furno, "Condensation of Vapor Mixtures. 1. Nonequilibrium Models and Design Procedures", *Ind. Eng. Chem. Process Des. Dev.*, 25, 83, 1986.

115. Toor, H.L., and J.K. Burchard, "Plate Efficiencies in Multicomponent Distillation", *AIChE J.*, 6(2), 202, 1960.

116. Treybal, R.E., **Liquid Extraction**, 2nd Ed. McGraw-Hill, New York, 1963.

117. Treybal, R.E., **Mass Transfer Operations**, 3rd Ed., McGraw-Hill, New York, 1980.

118. Underwood, A.J.V., Discussion in Guinot's paper, "Azeotropic Distillation in Industry", *Trans. Inst. Chem. Engrs.*, 16, 195, 1938.

119. Verhoye, L., and H. de Schepper, "The Vapour-Liquid Equilibria of the Binary, Ternary and Quaternary Systems Formed by Acetone, Methanol, Propan-2-ol, and Water", *J. Appl. Chem. Biotechnol.*, 23, 607, 1973.

120. Vickery, D.J., J.J. Ferrari and R. Taylor, "An 'Efficient' Continuation Method for the Solution of Difficult Equilibrium Stage Separation Process Problems", *Comput. Chem. Eng.*, 12(1), 99, 1988.

121. Warner, J.J. and I.J. Harris, "Design of Multi-Component Solvent Extraction Systems", *Chem. Eng. Res. & Des.*, 65(3), 261, 1987.

122. Yu. P., I.M. Elshayal, and B.C.Y. Lu, "Liquid-liquid-vapor Equilibria in the Nitrogen-methane-ethane System", *Can. J. Chem. Eng.*, 47, 495, 1969.

123. Walraven, F.F.Y., and P.V. Van Rompay, "An Improved Phase-Splitting Algorithm", *Comput. Chem. Eng.*, 12(8), 777, 1988.

124. Wang, Jui C., and Wang, Yui H., **Foundations of Computer Aided Chemical Process Design**, R.S.H. Mah, and W.D. Seider (editors), AIChE, New York, 1981.

125. Zdonik S.B., and F.W. Woodfield, Section 9, **The Chemical Engineers Handbook** 3rd Edition (R.H. Perry, Editor), p629, 1950.

126. Zogg, M., Dissertation, ETH Zürich, 1972 cited by Gorak, 1985.

Appendices

A Stability of Liquid Mixtures

The criterion which determines whether or not the mixture will spontaneously split into two or more phases is called the criterion of material stability, sometimes called diffusional stability or intrinsic stability. According to thermodynamics, the Gibbs free energy of a system always tends to the minimum. That means the mathematical condition for the limit of the stable state is that the first derivative of the Gibbs energy with respect to the mole number at constant temperature and pressure is equal to zero and the second derivative is positive. Let us begin to investigate the behavior of the simplest mixture, a binary liquid mixture. For a stable mixture the following relations hold.

$$\frac{\partial G}{\partial x_1} = 0 \tag{A.1}$$

$$\frac{\partial^2 G}{\partial x_1^2} > 0 \tag{A.2}$$

Since

$$\Delta x_1 = -\Delta x_2$$

so

$$\frac{\partial G}{\partial x_2} = 0; \qquad \frac{\partial^2 G}{\partial x_2^2} > 0 \tag{A.3}$$

Figure A.1 is a diagram of the relationship between the molar Gibbs free energy, G, and composition, x, for a binary mixture with a miscibility gap shown in the upper figure; the lower figure shows the liquid phase diagram. The spinodal curve (dotted line) shown in the lower graph of Figure A.1 is a locus of the inflection points in the G vs. x curve (see the upper graph of Figure A.1). The area outside of binodal

curve corresponds to the stable state, only one homogeneous liquid phase exists; inside the spinodal curve is unstable, or intrinsical unstable, even to an infinitesimal change in the composition, in the strict sense. A mixture located in this area will split spontaneously into two liquid phases. The mixture with compositions in the area between the binodal and spinodal curves (the shaded area in the lower graph of Figure A.1) is called meta-stable. This type of mixture is stable to small fluctuations in composition and splits into two liquid phase with a macroscopic difference of mole number. It is observed from the upper graph of Figure A.1 that the convex curve of G vs. x responds to the stable mixture; the concave curve represents the unstable form.

For a multicomponent mixture the total Gibbs free energy is calculated by:

$$\mathrm{G_0} \equiv \sum_{p=1}^{\pi} \mathrm{G}^p(n^p, T, P) \tag{A.4}$$

where superscript p represents the different phase and n is mole number.

The Gibbs free energy of the multicomponent mixture is defined as:

$$\begin{aligned} \mathrm{G}^p &\equiv \sum_{i=1}^{c} n_i^p \left(\frac{\partial \mathrm{G}^p}{\partial n_i^p}\right)_{T,P,n'} \\ &= n^p G^p(x^0, T, P) \qquad for \qquad n' \neq n_i \end{aligned} \tag{A.5}$$

where G is the molar Gibbs free energy.

If a small fluctuation occurs in the system, the change of the Gibbs energy is

$$\delta G = G - G_0 \tag{A.6}$$

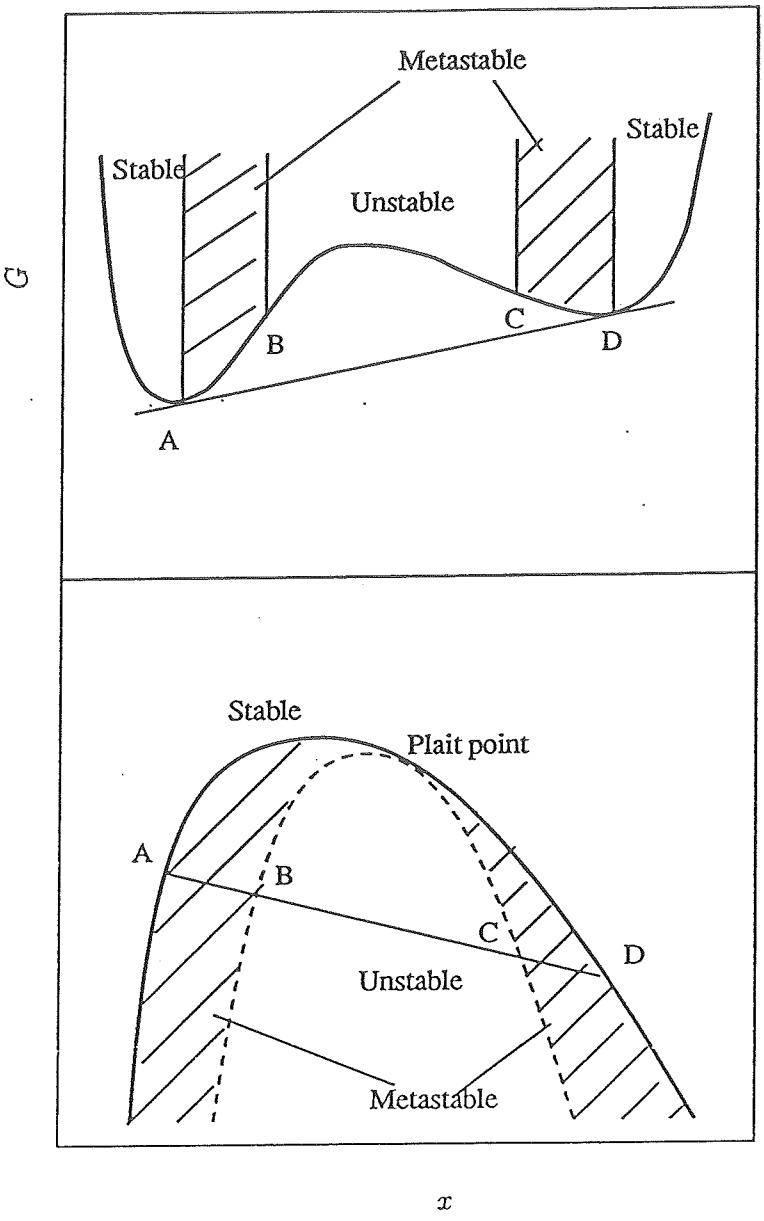

Figure A.1: Material stability of a liquid mixture.

According to the thermodynamic criteria:

If $\delta \mathrm{G} > 0$, the mixture is stable;

If $\delta \mathrm{G} < 0$, the mixture is unstable.

If a phase split occurs in response to this small fluctuation, the Gibbs free energy is estimated

$$\begin{aligned} \mathrm{G} &\equiv \sum_{p=I}^{\pi} n^p G^p(x^p, T, P) \\ &= n^I G(x + \epsilon^I, T, P) + n^{II} G(x + \epsilon^{II}, T, P) \end{aligned} \tag{A.7}$$

The molar Gibbs free energy G may be expanded in a Taylor series as

$$G(x+\epsilon) = G(x) + \sum_{i=1}^{c-1} \left(\frac{\partial G}{\partial x_i}\right)_{T,P,x'} \epsilon_i + \frac{1}{2} \sum_{i=1}^{c-1} \sum_{j=1}^{c-1} \left(\frac{\partial^2 G}{\partial x_i \partial x_j}\right)_{T,P,x'} \epsilon_i^I \epsilon_j^I + \cdots \tag{A.8}$$

Equations (A.1), (A.4), (A.7) and (A.8) may be substituted into (A.6) to give

$$\begin{aligned} \partial \mathrm{G} &= \frac{1}{2} \left(n^I + (n^I)^2/n^{II}\right) \sum_{i=1}^{c-1} \sum_{j=1}^{c-1} \left(\frac{\partial^2 G}{\partial x_i \partial x_j}\right)_{T,P,x'} \epsilon_i^I \epsilon_j^I \\ &= \frac{1}{2} \left(n^I + (n^I)^2/n^{II}\right) \epsilon^{I^T} [\varrho]\ \epsilon^I \end{aligned} \tag{A.9}$$

where

$$[\varrho_{ij}] = \left[\left(\frac{\partial^2 G}{\partial x_i \partial x_j}\right)_{T,P,x'}\right] \tag{A.10}$$

It follows from Equation (A.9) that if the matrix $[\varrho]$ is positive definite then δG should be positive for all small fluctuations, and the system is stable or metastable. Conversely if the matrix $[\varrho]$ is not positive definite, the system is intrinsically unstable.

B Overall Mass Transfer Coefficients for Multicomponent Systems

The calculation of the diffusion fluxes (J) of the liquid at the interface is presented by Krishna (1985) as:

$$\begin{aligned}(J) &= c_t^L[k^\circ]\Delta x \\ &= -c_t^L[\bar{\beta}^L][\bar{R}^L]^{-1}[\bar{\Gamma}^L](x - x^I)\end{aligned} \tag{B.1}$$

The interfacial molar fluxes (J) of vapor are obtained from

$$(J) = -c_t^V[\bar{\beta}^V][\bar{R}^V]^{-1}[\bar{\Gamma}^V](y^I - y) \tag{B.2}$$

If the vapor-liquid equilibrium relation can be linearized as

$$y_i^* = \sum_{j=1}^{c-1} \frac{\partial y_i^*}{\partial x_j} x_j + b_i \qquad i = 1, 2, \cdots, c-1 \tag{B.3}$$

Since

$$y_i^* = \frac{\gamma_i x_i P_i^0}{P_t} \qquad i, j = 1, 2, \cdots, c \tag{B.4}$$

Thus

$$\frac{\partial y^*}{\partial x_j} = K_i^{eq} \bar{\Gamma}_{ij}^L \qquad i, j = 1, 2, \cdots, c-1 \tag{B.5}$$

where K_i^{eq} is the K-value defined by

$$\begin{aligned}K_i^{eq} &= \frac{y_i^*}{x_i} \\ &= \frac{\gamma_i P_i^0}{P_t} \qquad i = 1, 2, \cdots, c-1\end{aligned} \tag{B.6}$$

Substitute equations (B-5) and (B-6) into (B-3), then

$$(y^*) = [K^{eq}][\bar{\Gamma}^L](x) + (b) \tag{B.7}$$

where $[K^{eq}]$ is a diagonal matrix of equilibrium K-values. y_i^* is the equilibrium composition with the bulk liquid phase composition x_i.

At the interface, Equation (B.7) is rewritten as

$$(y^I) = [K^{eq}][\bar{\Gamma}^L](x^I) + (b) \tag{B.8}$$

Combining equations (B.7) and (B.8) yields

$$(y^* - y^I) = [K^{eq}][\bar{\Gamma}^L](x - x^I) \tag{B.9}$$

Substituting Equation (B.1) into (B.9), then, the following equation is given

$$\begin{aligned}(y^* - y^I) &= -\frac{[K^{eq}][\bar{\Gamma}^L][\bar{\Gamma}^L]^{-1}[\bar{R}^L][\bar{\beta}^L]^{-1}(J)}{c_t^L} \\ &= -\frac{[K^{eq}][\bar{R}^L][\bar{\beta}^L]^{-1}(J)}{c_t^L}\end{aligned} \tag{B.10}$$

The vapor phase can be recognized as ideal gas, so $[\bar{\Gamma}^V] = [I]$. Equations (B.2) can be rearranged as

$$(y^I - y) = -\frac{[\bar{R}^V][\bar{\beta}^V]^{-1}(J)}{c_t^V} \tag{B.11}$$